Universitat Autònoma de Barcelona

Departament de Bioquímica i Biologia Molecular

MILLORA DE LA DIAGNOSI NO INVASIVA DELS TUMORS CEREBRALS HUMANS

Mª Margarita Julià Sapé

Cerdanyola del Vallès, 6 de Setembre de 2006

Universitat Autònoma de Barcelona

Departament de Bioquímica i Biologia Molecular

MILLORA DE LA DIAGNOSI NO INVASIVA DELS TUMORS CEREBRALS HUMANS

Memòria presentada per na Mª Margarita Julià Sapé per a optar al grau de Doctor en Ciències Biològiques per la Universitat Autònoma de Barcelona

Aquest treball ha estat realitzat al Departament de Bioquímica i Biologia Molecular de la Facultat de Ciències de la Universitat Autònoma de Barcelona, sota la direcció del Professor Dr. Carles Arús Caraltó.

Vist-i plau del director:

Carles Arús Caraltó *Mª Margarita Julià Sapé*

Cerdanyola del Vallès, 6 de Setembre de 2006

Acknowledgements / Agraïments / Agradecimientos

El meu agraïment al Professor Dr. Carles Arús per l'oportunitat que em va oferir de treballar al seu grup de recerca dins el projecte INTERPRET. També agraïr-li les oportunitats que m'ha continuat donant dia rere dia durant aquests anys i el seu incansable suport i convicció per tal de que la feina feta es convertís en feina escrita.

Thanks to the INTERPRET consortium: to all the scientists that engaged in the challenge and from I had the opportunity to learn.

Al Dr. Carles Majós pel seu temps, la seva generositat a l'hora de compartir els seus coneixements, el seu esperit crític i el seu fantàstic sentit de l'humor. El meu agraïment també a la resta de l'equip de l'IDI Bellvitge per la seva acollida durant els mesos en que vaig treballar físicament al seu centre en el projecte MEDIVO.

A en Miquel Cabañas: la seva generositat científica i humana van fer possible que només arribar al GABRMN aviat comencés a ser un membre productiu del grup. Gràcies per tantes idees, consells, solucions i converses. Al Dr. Dionisio Acosta: algunas de las más originales ideas de esta tesis son consecuencia de improductivas discusiones sobre nada en particular y todo en general que generaron preguntas aparentemente inútiles- en realidad las más relevantes.

Thanks to Dr. Pieter Wesseling and all the altruistic time devoted on the phone helping shape up and painstakingly revising one of the manuscripts of this thesis. Thanks to Professor John R. Griffiths, which gave perspective and just the right sentences to several draft papers, not only in this thesis. Gràcies al Dr. Àngel Moreno, al Dr. Jesús Pujol, al Dr Juan José Acebes pels seus comentaris crítics, orientacions i coneixements.

Gràcies a tots els companys del laboratori: A la Dra. Ana Paula Candiota, a la Maria Rosa Quintero, a la Indira Coronel, a en Rui Simoes, a en Daniel Valverde, i als nous companys: en Jorge Luis Zapata, en Sergi Torralba, l'Ivan Olier, en Raúl Cruz, i en Tiago Ferronha. Als companys que han continuat la seva carrera professional a d'altres llocs: a en Guillem Mercadal, a la Katja Schustakowitz, al Dr. Mohamed Zakari, a la Dra. Yolanda Pérez, a la Dra. Maria Gisele dos Santos, a en Jordi Nebot, a en Lluis Martí, a en Jordi Montero i a l'Eva Calpe. A cadascun de tots ells, gràcies per fer que el laboratori sigui un lloc molt agradable al qual anar a treballar cada matí, i per endolcir molts dies amb l'excusa d'una celebració. A Mariola Mier, compañera de fatigas en el cierre de las bases de datos de INTERPRET.

I als meus pares. Sense el seu incondicional suport, rès del que hi ha escrit a continuació hagués estat possible.

INDEX

Table index

Figure index

LIST OF ABBREVIATIONS

ν *: Precession frequency*

σ *: shielding factor*

^{13}C: carbon 13

1D: monodimensional

^{1}H: Proton

1H-MRS: proton magnetic resonance spectroscopy

2D: two dimensional

^{31}P:phosphrous 31

3D: three dimensional

AUC: area under the curve

B: Effective magnetic field

B_{ext}: External magnetic field

B_{int}: Internal magnetic field

CDP: Centre Diagnòstic Pedralbes

CH_2: methylene

CH_3: methyl

Cr: creatine

CSF: cerebrospinal fluid

CSI: chemical shift imaging

CT: computed tomography

DBMS: database managing system

DFT: discrete Fourier transform

DMS: data manipulation software

DSS: decision support system

DWI: diffusion weighted imaging

eTUMOUR: *Web accessible MR decision support system for brain tumour diagnosis and prognosis, incorporating in vivo and ex vivo genomic and metabolomic data*

EU: European Union

FFT: fast Fourier transform

FID: free induction decay

FLAIR: fluid-attenuated inversion-recovery

fMRI: functional MRI

GABA: gamma aminobutyric acid

GE: General Electric

Gln: glutamine

Glu: glutamate

Glx: glutamine and glutamate

GUI: graphical user interface

HR-MAS: high-resolution magic angle spinning

Hz: Hertz

iDB: INTERPRET database

IDI: Institut de Diagnòstic per la Imatge

INTERPRET: International Network for Pattern Recognition of Tumours Using Magnetic Resonance

IST: Information Society Technologies

LDA: linear discriminant analysis

MANOVA: multivariate analysis of variance

mI: myoinositol

MR: magnetic resonance

MRA: magnetic resonance angiography

MRI: magnetic resonance imaging

MRS: Magnetic Resonance Spectroscopy

ms: milliseconds

MV: multivoxel

NAA: N-acetyl aspartate

N-$(CH_3)_3$: trymethylamine group

NMR: Nuclear Magnetic Resonance

NPV: negative predictive value

PCr: phosphocreatine

PET: positron emission tomography

PNET: primitive neuroectodermal tumour

ppm: part per million

PPV: positive predictive value

PR. pattern recognition

PRESS: point resolved spectroscopy

QDA: quadratic discriminant analysis

ROC: receiver operating characteristic

SE: sensitivity

SNR: signal-to-noise ratio

SP: specificity

SQL: structured query language

STEAM: stimulated echo acquisition mode

SV: single voxel

SV-40: simian virus 40

SVS: single voxel spectroscopy

T: Tesla

T_1: spin-lattice relaxation time constant

T2: spin-spin relaxation time constant

TE: echo time

TR: recycling time

TSP: 3-trimetilsylil [2,2,3,3-^{2}H] sodium propionate

WBW: water bandwidth

WHO: World Health Organisation

1. OUTLINE

This PhD thesis deals with the applicability of magnetic resonance spectroscopy (MRS) to brain tumour diagnosis. The work discussed in it is a consequence of its author's work in the EU-IST-funded INTERPRET project (IST-1999-10310, <http://azizu.uab.es/INTERPRET>) and in the MEDIVO project, funded by the Spanish Ministry of Science (SAF 2002-00440).

The dissertation is structured as follows: After a short ***Introduction*** covering the main areas of interest, the purpose and main results of INTERPRET are presented, as well as limitations and questions remaining unsolved after the project's end. Next, the ***Objectives*** of the work are presented. ***Articles*** 1, 2 and 3 constitute the body of methods and results. A ***General Discussion*** section wraps up the main results, shortly giving some general considerations that have not been discussed in detail in the individual articles.

2. ABSTRACT

2.1. ABSTRACT IN ENGLISH LANGUAGE

***Purpose**: To improve the non-invasive characterisation of brain tumours with ^{1}H-MRS (proton magnetic resonance spectroscopy).*

For this, three studies were performed, with the following objectives: 1) To generate an Internet-accessible database that contains validated in-vivo MR spectra and clinical data of brain tumour patients. 2) To determine the influence of the TE used in brain tumour classification by comparing the performance of spectra obtained at two different TE (30 ms and 136 ms). 3) To estimate the accuracy of routine MRI in the classification of brain tumours both in terms of cell type and grade of malignancy.

***Methods**: Study 1) All data from patients entering the INTERPRET project (International Network for Pattern Recognition of Tumours Using Magnetic Resonance, http://azizu.uab.es/INTERPRET) were stored in a web-accessible database (iDB) and selected using its query functionality. Criteria for selection were that the case had a single voxel (SV) short-echo (20-32 ms) 1.5 T spectrum acquired from a nodular region of the tumour, that the voxel had been positioned in the same region as where subsequent biopsy was obtained, that the short-echo spectrum had not been discarded because of acquisition artefacts or other reasons, and that a histopathological diagnosis was agreed among a committee of*

neuropathologists. When the spectra were obtained from normal volunteers or were of abscesses or clinically proven metastases, biopsy was not required.

Study 2) One hundred fifty-one studies of patients with brain tumours from the MEDIVO project (37 meningiomas, 12 low grade astrocytomas, 16 anaplastic astrocytomas, 54 glioblastomas, and 32 metastases) were retrospectively selected from a series of 378 consecutive examinations of brain masses. Single voxel proton MR spectroscopy at TE 30 ms and 136 ms was performed with point-resolved spectroscopy in all cases. Fitted areas of nine resonances of interest were normalized to water. Tumours were classified into four groups (meningioma, low grade astrocytoma, anaplastic astrocytoma, and glioblastoma-metastases) by means of linear discriminant analysis. The performance of linear discriminant analysis at each TE was assessed by using the leave-one-out method.

Study 3) Retrospective assessment of agreement between radiological classification and histopathological diagnosis was carried out using records of 393 brain tumour patients stored in a multi-centre database from the INTERPRET project. An ontology for agreement definition was devised. Each tumour category was bilaterally compared to the corresponding histopathological diagnoses by dichotomisation. Sensitivity (SE), Specificity (SP), Positive (PPV) and Negative Predictive (NPV) values and their Wilson's 95% confidence intervals (CI) were calculated.

***Results**: Study 1) A subset of 304 cases (22 normal volunteers and 282 tumour patients) was obtained. These cases were migrated to a web-*

accessible database (validated-DB). Study 2) Tumour classification was slightly better at short TE (123 [81%] of 151 cases correctly classified) than at long TE (118 [78%] of 151 cases correctly classified). Meningioma was the only group that showed higher sensitivity and specificity at long TE. Improved results were obtained when both TE were considered simultaneously: the suggested diagnosis was correct in 105 (94%) of 112 cases when both TE agreed, whereas the correct diagnosis was suggested by at least one TE in 136 (90%) of 151 cases. Study 3) In routine radiological reporting of MRI examinations, tumour types and grades were classified with high SP (85.2-100%); SE varied, depending on type and grade, alone or in combination. Recognition of broad categories (neuroepithelial, meningeal) was highly sensitive whereas it diverged when both detailed type and grade were considered, being highest in low-grade meningioma (SE=100%, CI=96.2-100.0%) and lowest in high-grade meningioma (SE=0.0%, CI=0.0-65.8%) and low-grade oligodendroglioma (SE=15%, CI=5.2-36.0%). In neuroepithelial tumours SE was inversely related to precision in reporting of grade and cellular origin; "glioma" was a frequent radiological classification associated with a higher SE in the corresponding category. PPV varied among categories being in general above their prevalence in this dataset. NPV was high in all categories (69.8-100%).

***Conclusions**: The validated-DB complies with ethics regulations and represents the population studied. It is accessible by neuroradiologists willing to use information provided by MRS to help in the non-invasive*

diagnosis of brain tumours. Short TE provides slightly better tumour classification, and results improve when both TE are considered simultaneously. Meningioma was the only tumour group in which long TE performed better than short TE. PPV and NPV provided for routine MRI characterisation of brain tumours may be used as estimates of post-test probabilities of diagnostic accuracy achieved by MRI in the database studied. The need for non-invasively increasing SE in categorization of most brain tumour types while retaining high SP, especially in the differentiation of high and low-grade glial tumour classes has been targeted.

2.2. RESUM EN LLENGUA CATALANA

***Propòsit**: Millorar la caracterització no invasiva dels tumors cerebrals mitjançant la tècnica de l'espectroscopia de ressonància magnètica de protó.*

Per a assolir aquest objectiu, es van realitzar tres estudis, amb els següents objectius: Estudi 1) Generar una base de dades accessible per Internet, que contingui dades clíniques i espectroscòpiques completament validades de pacients afectats per tumors cerebrals. Estudi 2) Determinar la influència del temps d'eco utilitzat en l'adquisició en la posterior classificació dels espectres de tumours cerebrals humans. Per això es va comparar l'encert obtingut en la classificació tumoral utilitzant dos temps d'eco diferents (30 ms and 136 ms). Estudi 3) Estimar l'encert de la

interpretació de les imatges de ressonància en la classificació dels tumors cerebrals, tant en termes de tipus com de grau de malignitat tumoral.

***Mètodes**: Estudi 1) Totes les dades dels pacients que van entrar al projecte INTERPRET (International Network for Pattern Recognition of Tumours Using Magnetic Resonance, http://azizu.uab.es/INTERPRET) es van guardar a una base de dades accessible per Internet (iDB). Les dades dels pacients es van seleccionar utilitzant la interfície de preguntes de la base de dades. Els criteris que es van seguir van ser que el cas tingués un espectre adquirit a 1.5 T mitjançant la tècnica de volum senzill i temps d'eco curt (20-32 ms) sobre una àrea nodular del tumor, que el volum d'adquisició hagués estat posicionat dins de la mateixa regió de la qual es va prendre posteriorment la biòpsia diagnòstica, i que l'espectre a temps d'eco curt no hagués estat descartat per artefactes d'adquisició o altres raons, i que un comitè de neuropatòlegs hagués sin arribat a consens diagnòstic. Quan els espectres es van obtenir de voluntaris normals, o éren d'abscessos o de metàstasis provades clínicament, no es va requerir biòpsia.*

Estudi 2) Es van sel·leccionar de manera retrospectiva cent cinquanta-un estudis de pacients amb tumors cerebrals (37 meningiomas, 12 astrocitomes de baix grau, 16 astrocitomes d'alt grau, 54 glioblastomes i 32 metastasis) d'una sèrie de trescents setanta-vuit exàmens de masses cerebrals anòmales d'un dels centres col.laboradors d'INTERPRET dintre del projecte MEDIVO. Es va realitzar espectroscopia de volum senzill a temps d'eco 30 ms i 136 ms en tots els casos. Es van normalitzar les

àrees integrades de nou ressonàncies d'interès. Els espectres dels tumors es van classificar mitjançant anàlisi discriminant en quatre grups: meningioma, astrocitoma de baix grau, astrocitoma d'alt grau i glioblastomes juntament amb metastasis. Es va aval.luar el resultat de l'anàlisi discriminant a cadascun dels temps d'eco utilitzant el mètode de deixar un cas fora.

Estudi 3) L'acord entre la classificació radiològica i el diagnòstic histopatològic es *va aval·luar retrospectivament, utilitzant dades retrospectives de trescents noranta-tres pacients de tumors cerebrals que estàven guardats a la base de dades multicèntrica del projecte INTERPRET. Es va crear una ontologia per a poder definir l'acord entre diagnòstics. Cada categoria tumoral es va comparar bilateralment amb els diagnòstics histopatològics corresponents. Es van calcul.lar els valors de sensibilitat, especificitat, valors predictius positiu i negatiu, juntament amb els intervals de confiança del 95% de Wilson.*

***Resultats**: Estudi 1) Es va obtenir un subgrup de trescents quatre casos (vint-i-dos voluntaris normals i dos-cents vuitanta-dos pacients). Aquests casos es van migrar a una altra base de dades accessible per internet (base de dades validada). Estudi 2) La classificació dels tumors va ser lleugerament millor a temps d'eco curt (123 [81%] de 151 casos classificats correctament) que a temps d'eco llarg (118 [78%] de 151 casos classificats correctament). Els meningiomes van ser l'únic grup pel qual es va obtenir una millor sensibilitat i especificitat a temps d'eco llarg. Els resultats van millorar quan ambdós temps d'eco es consideràven*

simultàniament: el diagnòstic suggerit va ser correcte en 105 (94%) de 112 casos quan el resultat predit a ambdós temps d'eco era el mateix. Es va suggerir el diagnòstic correcte almenys a un temps d'eco en 136 (90%) casos de 151. 3) Quan els radiòlegs informen estudis d'imatge, són molt específics (85.2-100%) a l'hora de caracteritzar el grau i el tipus de tumor. La seva sensibilitat varia depenent del tipus i el grau, separadament i en combinació. En les categories àmplies (neuroepitelial, llinatge meningeal) vàren ser molt sensibles mentre que quan es va considerar còm s'informava el tipus detallat i el grau la sensibilitat variava, essent la més alta en els meningiomes de baix grau (sensibilitat 100%, intèrval de confiança, 96.2-100.0%) i la més baixa pels meningiomes d'alt grau (sensibilitat, 0.0%, intèrval de confiança, 0.0-65.8%) i els oligodendrogliomes de baix grau (sensibilitat, 15%, intèrval de confiança, 5.2-36.0%). La sensibilitat en la detecció dels tumors d'orígen neuroepitel.lial es va relacionar de manera inversa amb la precisió en la manera de descriure el grau i l'orígen cel.lular del tumor. "Glioma" era una classificació radiològica freqüent, associada a una més alta sensibilitat a la seva categoria corresponent. El valor predictiu positiu va variar entre categories, assolint en general valors per sobre de la prevalença dels tumors respectius en aquesta base de dades. El valor predictiu negatiu va ser alt a totes les categories analizades (69.8-100%).

***Conclusions**: La base de dades validada compleix amb les regul.lacions ètiques i és representativa de la població que estudia. És accessible a neuroradiòlegs arreu del món que vulguin utilitzar la informació que dóna*

l'espectroscopia per tal d'ajudar en el diagnòstic no invasiu dels tumors cerebrals.

El temps d'eco curt dóna una classificació lleugerament millor que el temps d'eco llarg, i els resultats milloren quan ambdós temps d'eco es consideren de manera simultània. Els meningiomes són l'únic grup tumoral en el qual el temps d'eco llarg és lleugerament millor que el temps d'eco curt.

Els valors predictius positiu i negatiu que es van obtenir es poden utilitzar com a estimadors de les probabilitats a posteriori per a la caracterització dels tumors cerebrals mitjançant les imatges de ressonància en la base de dades INTERPRET. A més a més, es va fer palesa la necessitat d'augmentar la sensibilitat en la categorització de la majoria de tumors cerebrals, mantenint l'alta especificitat, especialment en la diferenciació entre tumors glials d'alt i baix grau, especialment amb tècniques associades a la imatge, com l'espectroscopia de ressonància magnètica de protó.

2.3. RESÚMEN EN LENGUA CASTELLANA

***Objetivo**: Mejorar la caracterización no invasiva de los tumores cerebrales por medio de la técnica de espectroscopía de resonancia magnética de protón.*

Para alcanzar este objectivo, se realizaron tres estudios, con los siguientes objectivos: Estudio 1) Generar una base de datos accesible por Internet,

que contenga datos clínicos y espectroscópicos completamente validados de pacientes afectados por tumores cerebrales. Estudio 2) Determinar la influencia del tiempo de eco utilizado en la adquisición en la posterior clasificación de los espectros de tumores cerebrales humanos. Para ello se comparó el acierto obtenido en la clasificación tumoral utilizando dos tiempos de eco diferentes (30 ms y 136 ms). Estudio 3) Estimar el acierto en la interpretación de las imágenes de resonancia para la clasificación de los tumores cerebrales, tanto en términos de tipo como de grado de malignidad tumoral.

***Métodos**: Estudio 1) Todos los datos de los pacientes que entraron en el proyecto INTERPRET (International Network for Pattern Recognition of Tumours Using Magnetic Resonance, http://azizu.uab.es/INTERPRET) se guardaron en una base de datos accesible por Internet (iDB). Estos datos se seleccionaron mediante la interfaz de preguntas de la base de datos. Los criterios que se siguieron fueron que el caso tuviera un espectro adquirido a 1.5 T mediante la técnica de volumen único y a tiempo de eco corto (20-32 ms) sobre una area nodular del tumor, que el volumen de adquisición hubiera sido posicionado en la misma región de la cual se tomó posteriormente la biopsia diagnóstica, y que el espectro a tiempo de eco corto no hubiera sido descartado por artefactos de adquisición u otras razones, y que un comité de neuropatólogos hubiera alcanzado consenso diagnóstico. Cuando los espectros se obtuvieron de voluntarios normales, o eran de abscesos o de metástasis probadas clínicamente no se requirió biopsia.*

Estudio 2) Se seleccionaron de forma retrospectiva ciento cincuenta y un estudios de pacientes con tumores cerebrales (37 meningiomas, 12 astrocitomas de bajo grado, 16 astrocitomas de alto grado, 54 glioblastomas y 32 metástasis) de una serie de trescientos setenta y ocho exámenes de masas cerebrales anómalas realizados dentro del proyecto MEDIVO . Se realizó espectroscopía de volumen único a tiempo de eco 30 ms y 136 ms en todos los casos. Se normalizaron las áreas integradas de nueve resonancias de interés. Los tumores se clasificaron en cuatro grupos mediante análisis discriminante: meningioma, astrocitoma de bajo grado, astrocitoma de alto grado y glioblastomas juntamente con metástasis. Se evaluó el resultado del análisis discriminante a cada tiempo de eco mediante el método de dejar un caso fuera.

Estudio 3) Se evaluó retrospectivamente el acuerdo entre la clasificación radiológica y el diagnóstico histopatológico, utilizando datos retrospectivos de trescientos noventa y tres pacientes de tumores cerebrales que estaban guardados en la base de datos de INTERPRET (iDB). Se creó una ontología para poder definir acuerdo entre diagnósticos. Cada categoría tumoral se comparó bilateralmente con los diagnósticos histopatológicos correspondientes. Se calcularon los valores de sensibilidad, especificidad, valores predictivos positivo y negativo, y también sus intervalos de confianza del 95% de Wilson.

***Resultados**: Estudio 1) Se obtuvo un subgrupo de trescientos cuatro casos (veintidos voluntarios normales y doscientos ochenta y dos pacientes). Estos casos se migraron a otra base de datos similar (base de*

datos validada). Estudio 2) La clasificación tumoral fue ligeramente mejor a tiempo de eco corto (123 [81%] de 151 casos clasificados correctamente) que a tiempo de eco largo (118 [78%] de 151 casos clasificados correctamente). Los meningiomas fueron el único grupo para el que la clasificación fue más sensible y específica a tiempo de eco largo. Los resultados mejoraron significativamente cuando ambos tiempos de eco se consideraban simultaneamente: el diagnóstico sugerido fue correcto en 105 (94%) de 112 casos cuando el resultado predicho a ambos tiempos de eco era el mismo. Se sugirió el diagnóstico correcto al menos en uno de los dos tiempos en 136 (90%) casos de 151. Estudio 3) Cuando los radiólogos informan estudios de imagen de resonancia magnética, son altamente específicos (85.2-100%) en la caracterización del grado y tipo de tumor. Su sensibilidad es variable dependiendo del tipo y grado, separadamente y en combinación. En las categorías amplias (neuroepitelial, estirpe meníngea) fueron muy sensibles mientras que cuando se consideró la manera de informar el tipo detallado y el grado, la sensibilidad era variable, siendo la más alta para los meningiomas de bajo grado (sensibilidad 100%, intervalo de confianza, 96.2-100.0%) y la más baja en los meningiomas de alto grado (sensibilidad, 0.0%, intervalo de confianza, 0.0-65.8%) y en los oligodendrogliomas de bajo grado (sensibilidad, 15%, intervalo de confianza, 5.2-36.0%). La sensibilidad en la detección de los tumores de orígen neuroepitelial se relacionó inversamente con la precisión al describir el grado y el orígen celular del tumor. "Glioma" fue una clasificación radiológica frecuente, asociada a una

más alta sensibilidad en su categoria correspondiente. El valor predictivo positivo varió entre categorías, alcanzando en general valores por encima de la prevalencia de los tumores respectivos en esta base de datos. El valor predictivo negativo fue alto para todas las categorías analizadas (69.8-100%).

***Conclusiones**: La base de datos validada cumple con las regulaciones éticas y representa la población que estudia. Es accesible a neuroradiólogos de todo el mundo que deseen utilizar la información espectroscópica en el diagnóstico no invasivo de los tumores cerebrales.*

El tiempo de eco corto provee una clasificación ligeramente mejor que el tiempo de eco largo, y los resultados mejoran cuando se consideran los dos tiempos de eco de forma simultánea. Los meningiomas son el único grupo tumoral para el cual el tiempo de eco largo es ligeramente mejor que el tiempo de eco corto.

Los valores predictivos positivo y negativo para el diagnóstico por imágenes de resonancia que se obtuvieron pueden utilizarse como estimadores de las probabilidades a posteriori para la caracterización de los tumores cerebrales en la base de datos INTERPRET. Además, se puso en evidencia la necesidad de aumentar la sensibilidad en la categorización de la mayoría de tumores cerebrales, manteniendo la alta especificidad, especialmente en la diferenciación entre tumores gliales de alto y bajo grado, especialmente mediante técnicas como la espectroscopía de resonancia magnética de protón.

3. INTRODUCTION

3.1 NUCLEAR MAGNETIC RESONANCE SPECTROSCOPY

3.1.1. Physics of nuclear magnetic resonance spectroscopy

The phenomenon of nuclear magnetic resonance (NMR) was described for the first time by Bloch [1] and Purcell [2]. Some atoms have the property of absorbing radiofrequency energy and re-emitting it during the transition to their original state when they are placed in a magnetic field. This property is determined by another property: the spin of these nuclei. As nuclei are electrically charged, the spin generates a magnetic field oriented along the spinning axis, in the form of magnetic dipole. The resonance frequency of this process at which energy can be absorbed is called precession frequency (ν) and it is directly proportional to the effective magnetic field (B) that the nucleus perceives, as defined by the Larmor Law in *Equation 1*:

(*Equation 1*) $$\nu = \gamma \cdot \frac{B}{2\Pi}$$

Where γ is the giromagnetic constant, which is characteristic of each nucleus; *B* is the magnetic field, which is the result of the effect of the magnetic field generated by the magnet (B_{ext}) and the internal magnetic field (B_{int}) induced by charges in movement that constitute part of the

1 Bloch F, Hansen WW, Packard M. The nuclear induction experiment. Phys Rev 1946; 70: 474-485.
2 Purcell EM, Torrey HC, Pound RV. Resonance absorption by nuclear magnetic moments in a solid. Phys Rev 1946; 69: 37-38.

molecules, among other possible origins. There is a proportionality between them, defined by a constant σ or "shielding factor", where:

(*Equation 2*) $$B_{int} = \sigma \cdot B_{ext}.$$

When γ and B_{ext} are constant, ν will depend of σ. This σ value varies depending on the structure of each molecule. In this way, ν will be characteristic of each chemical group in a given molecule and the changes in electronic shielding of the nucleus of interest. As a result, magnetic resonance gives the possibility of simultaneously detecting chemical compounds present in a given sample.

The nucleus that has been more widely used in NMR is the proton (^{1}H). The precession frequency of ^{1}H is normally given in adimensional units of parts per million (ppm). This is obtained from the calculation of the chemical shift of the resonance of interest with respect to a reference resonance, as shown in *Equation 3*:

(*Equation 3*) $$\delta = \left[(\nu_{pA} - \nu_{pR}) / \nu_{pR}\right] \cdot 10^6$$

Where ν_A is the ν of metabolite A and ν_R is the ν of the reference molecule. In the case of ^{1}H, a common reference substance is 3-trimetilsylil [2,2,3,3-^{2}H] sodium propionate (TSP) which is given a 0 ppm chemical shift position. It is also common practice to use indirect internal references for in-vivo studies (e.g. water at 4.75 ppm at 37ºC or the N-CH_3 group of phosphocreatine and creatine at 3.03 ppm). Once a spectrum is obtained, the position (in the frequency axis) of each resonance can be compared with the position of known chemicals, and the

amount of substance at the postion can be estimated by measuring its resonance area.

After the radiofrequency pulses have been applied, the nuclei start to "relax". The relaxation process in resonance is described by the time constants T_1 (spin-lattice constant) and T_2 (spin-spin constant). These parameters are sample (e.g. tissue) dependent, introducing the possibility to differentiate tissue types in the human body. T_1 and T_2 are related to physical interaction phenomena (e.g. rotational freedom) in the tissue.

3.1.2. In-vivo MR spectroscopy

For performing in-vivo MR spectroscopy it is of utmost importance to accurately obtain the NMR signal from a defined volume of tissue within an anatomical region of the body. The so-called "localisation techniques" are used for this purpose. These can be divided into two types, single volume (voxel) (SV) techniques, and multi-voxel techniques (MV), also named "chemical shift imaging" (CSI) techniques. In SV spectroscopy, a spectrum is acquired from a small volume of tissue defined by the intersection of three orthogonal planes. MV localization techniques can be in one dimension (1D), in two (2D) or in three (3D) dimensions and produce a "matrix" of contiguous voxels. In clinical MRS, single voxel spectroscopy (SVS) and 2D and 3D MV or chemical shift imaging (CSI) are normally used.

For volume definition in SV, one approach is to excite only the volume of interest with frequency selective radiofrequency pulses. This can be

achieved in *in-vivo* spectroscopy in different ways, among which there are the stimulated echo acquisition mode (STEAM) [3] or the point resolved spectroscopy (PRESS) [4]. In both STEAM and PRESS, three selective radiofrequency pulses are applied, but they differ in other parameters, such as the sequence timing and the placement of the pulses. From a practical point of view, in *in-vivo* MR spectroscopy, spectra acquired using a PRESS sequence will have double signal-to-noise than those acquired using STEAM sequences and will thus be preferable for comparable echo times when provided by the scanner manufacturer.

3.1.3. Analysis of spectral data

Once a spectrum signal has been acquired, a recording of the signal voltage against time (what is called, in the "time domain") is available, e.g. a graph showing an interpherogram of the amplitude and phase of the sine waves that make up the signal, and it is usually transformed into a signal in the "frequency domain". In digital spectral analysis, a computer algorithm called fast Fourier transform (FFT) is used [5]. It calculates in a fast way the discrete Fourier transform (DFT) of a time domain signal, transforming between the time and the frequency domains [6]. The frequency signal that is obtained after the FFT is known as the MR spectrum. A typical ^{1}H MRS signal recorded from a living tissue will be

3 Frahm J, Bruhn H, Gyngell ML, Merboldt KD, Hanicke W, Sauter. R. Localized high-resolution proton NMR spectroscopy using stimulated echoes: initial applications to human brain in vivo. Magn Reson Med. 1989; 9(1): 79-93.
4 Bottomley PA.Spatial localization in NMR spectroscopy in vivo. Ann N Y Acad Sci. 1987;508:333-48.
5 James W. Cooley and John W. Tukey. An algorithm for the machine calculation of complex Fourier series. Math Comput. 1965; 19: 297–301.
6 Carl Friedrich Gauss. Nachlass: Theoria interpolationis methodo nova tractata. Werke band, Königliche Gesellschaft der Wissenschaften. 1866; 3: 265–327.

called a free induction decay (FID) and it will consist of a large signal from water and several small signals from the metabolites that are in solution. The shape of a FID is that of a decaying sinusoid function representing the water signal, with superimposed sinusoids that represent the contribution from the metabolite signals. Additional data processing is needed in order to remove the residual water signal and to isolate the signals from metabolites. This can be done in the time or in the frequency domain, and several methods exist for that [7, 8, 9]. After Fourier transform, phase correction [10], subtraction of the water signal [11] baseline correction and additional phasing -if needed- are usually performed. If signals are being quantitated, a variety of methods also exist, and among the most commonly used there are the AMARES algorithm [12] which is included in the jMRUI software package [13], and the LC model [14].

3.1.4. Biochemical origin of magnetic resonance spectra

Once an MR spectrum has been processed it has to be interpreted, which usually requires assigning the contribution of a biochemical substance to

7 Mierisova S, Ala-Korpela M. MR spectroscopy quantitation: a review of frequency domain methods. NMR Biomed. 2001; 14(4): 247-259.
8 in 't Zandt H, van Der Graaf M, Heerschap A. Common processing of in vivo MR spectra. NMR Biomed. 2001; 14(4): 224-232.
9 Vanhamme L, Sundin T, Van Hecke P, Van Huffel S, Pintelon R. Frequency-selective quantification of biomedical magnetic resonance spectroscopy data. J Magn Reson. 2000; 143(1): 1-16.
10 Klose U. In vivo proton spectroscopy in presence of eddy currents. Magn Reson Med. 1990; 14(1): 26-30.
11 Laudadio T, Mastronardi N, Vanhamme L, Van Hecke P, Van Huffel S. Improved Lanczos algorithms for blackbox MRS data quantitation. J Magn Reson. 2002; 157(2): 292-297.
12 Vanhamme L, van den Boogaart A, Van Huffel S. Improved method for accurate and efficient quantification of MRS data with use of prior knowledge. J Magn Reson. 1997; 129(1) :35-43.
13 Naressi A, Couturier C, Castang I, de Beer R, Graveron-Demilly D. Java-based graphical user interface for MRUI, a software package for quantitation of in vivo/medical magnetic resonance spectroscopy signals. Comput Biol Med. 2001; 31(4): 269-286.
14 Provencher SW. Automatic quantitation of localized in vivo 1H spectra with LCModel. NMR Biomed. 2001; 14(4): 260-264.

each of the peaks or signals observed in the spectrum, i.e. peak identification. This is usually performed using readily available chemical-shift information from high-resolution MR spectroscopy (performed at high field intensities with model solutions) [15, 16] and from phantoms (model solutions) placed in the same 1.5 T magnets used for *in-vivo* studies. Table 1 Shows the major metabolites that can be detected in human brain and human brain tumours and other pathologies (e.g. abscesses) *in-vivo* at 1.5 T with magnetic resonance.

A brief outline of the most important metabolites that can be identified in the human brain and human brain pathological brain follows below.

The methyl (CH_3) group of N-acetyl groups, at 2.02 ppm. This signal is basically contributed by N-acetyl aspartate (NAA). The signal from the methylene (CH_2) group of NAA appears at 2.61 ppm. The CH_3 of Creatine and phosphocreatine (usually named as "total Cr") generate a signal at 3.03 ppm and the CH_2 can be observed at 3.93 ppm if good water suppression is achieved. Total Cr is considered stable enough under physiological conditions to be used as internal reference when reporting relative concentrations of other brain metabolites. The signal from Choline and other Choline-containing compounds such as Phosphocoline and Glycerophosphocholine appears at 3.21 ppm and is generated by the nine ^1H in the $(CH_3)_3$ group of Choline. The signal from the CH_3 of Lactate

15 Localized high-resolution proton NMR spectroscopy using stimulated echoes: initial applications to human brain in vivo. Magn Reson Med. 1989; 9(1): 79-93.

16 Merboldt KD, Hanicke W, Gyngell ML, Bruhn H, Frahm J. On the identification of cerebral metabolites in localized 1H NMR spectra of human brain in vivo. NMR Biomed. 1991; 4(2): 90-98.

appears centred at 1.33 ppm as an inverted doublet at TE 135-136 ms with STEAM or PRESS sequences due to J coupling phase modulation. It

Metabolite	(ν)ppm	Multiplicity
Mobile lipids	Several resonances from 0.5 to 5.40, the most detectable ones at 0.9, 1.3 and 2.0	Apparent singlets
Lactate	1.33	Doublet
Alanine	1.47	Doublet
Acetate	1.92	Singlet
N-acetyl aspartate	2.02	Singlet
Glutamate	2.10	Multiplet
Glutamine	2.14	Multiplet
Glutamate	2.35	Triplet
Succinate	2.42	Singlet
Glutamine	2.46	Triplet
N-acetyl aspartate, Glutamate, Glutamine	2.61	Quadruplet
Creatine	3.03	Singlet
Trimethylamine group-containing compounds (Choline, Phosphocholine, Glycerophosphocholine and others), generically labelled as "choline"	3.21	Singlet
Scyllo-Inositol	3.35	Singlet
Taurine, Glucose	3.43	Triplet
Myo-Inositol	3.55	Multiplet
Glycine	3.56	Singlet
Glutamate	3.77	Triplet
Glutamine	3.78	Triplet
Alanine	3.79	Quadruplet
Glucose	3.80	Singlet
Creatine	3.93	Singlet

Table 1 *Summary of the most important metabolite resonances that can be found in in-vivo ^{1}H spectra at 1.5 T in human brain (normal and pathologic). The ppm value given corresponds to the maximum peak intensity or the mean position in cases of doublets, triplets or quadruplets. Multiplicity is only observable in-vivo (i.e. at 1.5T for example) in certain cases (Lactate and Alanine).*

appears upright at short TE (20-35 ms) or at longer TE (272 ms). The CH_3 of Alanine is a doublet centred at 1.47 ppm. The signal also appears inverted at long TE (135-136 ms) and upright at short TE (20-35 ms). Glutamine (Gln) and Glutamate (Glu) are commonly referred as *Glx*. Their β-CH_2 and γ-CH_2 produce several peaks in the 2.0-2.46 ppm range and their α-CH group produce signals in the 3.6-3.8 ppm range. Gamma-aminobutyric acid (GABA) shows peaks at 1.9 ppm (β-CH_2), 2.3 ppm (α-CH_2) and 3.00 ppm (γ-CH_2)- this latter peak is usually masked by the Cr+PCr N-CH_3 peak. Glucose may produce two detectable peaks from the C1-C6 protons: at 3.43 and 3.80 ppm. There are other metabolites with short T2, which are scarcerly visible in the spectra at long TE. One example is Myo-Inositol (mI) at 3.55 ppm, with the CH protons on C1, C3, C4 and C6. Another mI resonance is detectable at 4.06 ppm. Resonances from NMR-visible mobile lipids, with peaks at 0.9 ppm (CH_3 of fatty acids) and 1.3 ppm ($(CH_2)_n$ of fatty acids)are also encountered in in-vivo spectroscopy of brain tumours, being more prominent with short TE sequences due to their T2.

Figure 1 shows some examples of ^1H spectra of normal and pathologic brain with metabolite assignments.

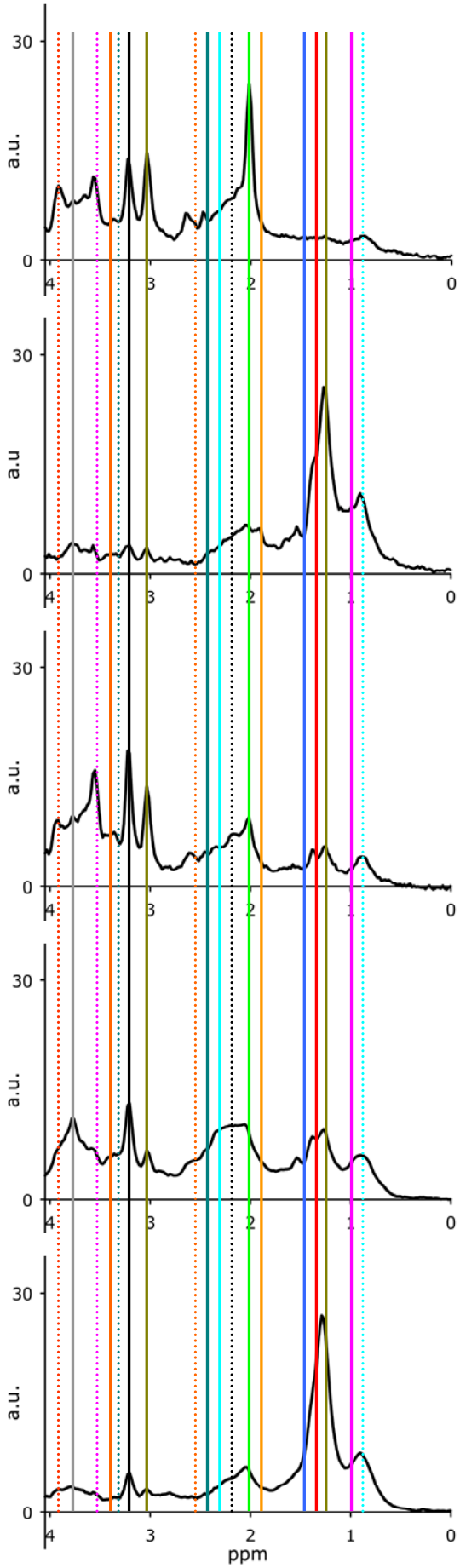
30
a.u.
0
4
3
2
1
0
ppm

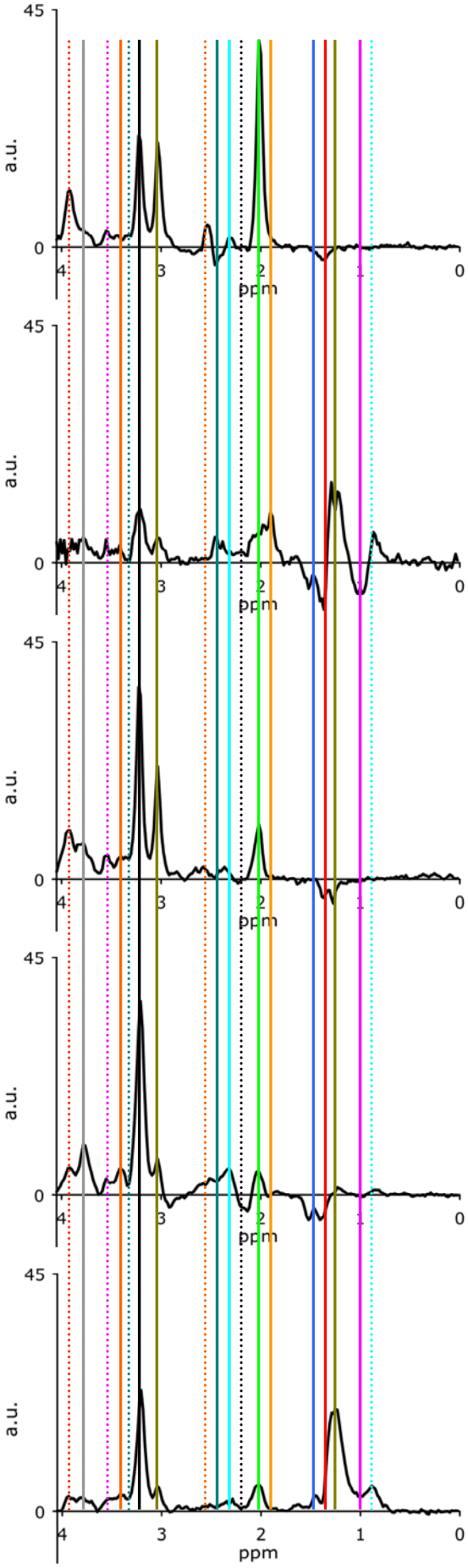
45
a.u.
0
4
3
2
1
0
ppm

***Figure 1**: Example of metabolite assignments for normal and pathologic human brain ^{1}H spectra. X axis: frequency axis in ppm. Y axis: arbitrary units. Left, short TE (20-32ms) spectra. Right: Long TE (136 ms) spectra. Top to bottom: Normal brain, abscess, Astrocytoma WHO grade II, Meningioma, Metastasis.. Coloured lines indicate the resonance frequencies for some relevant metabolites. Legend (from right to left): Discontinous light blue line: Mobile lipids and macromolecules at 0.9 ppm; Solid pink line: Aminoacids; Solid grey line: Mobile lipids and macromolecules at 1.3 ppm; Solid red line: Centre of the Lactate doublet; Solid dark blue line: Centre of the Alanine doublet; Solid dark yellow line: Acetate; Solid green line: N-acetyl-aspartate; Discontinous grey line: Glutamine and Glutamate; Solid light blue line:.Glutamine and Glutamate; Solid dark green line: Glutamine and Glutamate; Discontinous dark yellow line: Glutamine and Glutamate; Solid khaki line: Creatine; Solid black line: Choline-containing compounds (mainly Choline and Phosphocholine); Discontinous dark green line: Taurine; Solid orange line: Taurine and glucose; Discontinous pink line: Myo-Inositol and Glycine; Solid grey line: Glutamine, Glutamate and Alanine; Discontinous orange line: Creatine. Spectra graphs taken from [17]*

3.2. MAGNETIC RESONANCE IMAGING

In order to obtain an image, three orthogonal gradients in the magnetic field are applied to the object studied (for example, a human body). In this way, each spin system present in the object will experience a unique magnetic field that will allow locating its associated emitted signal. MR images are reconstructed from the entire object's ^{1}H signal, which is dominated by the water signal, and to a much lesser extent, by the fat

17 Tate AR, Underwood J, Acosta DM, Julià-Sapé M, et al. Development of a decision support system for diagnosis and grading of brain tumours using in vivo magnetic resonance single voxel spectra. NMR Biomed. 2006 (in press)

signals. In fact, the technique allows obtaining a picture of the ^{1}H in the water of an object "weighed" by its relative concentration and mobility. The rest of MR-visible metabolites present in tissues do not contribute significantly to the MR image signal due to their low proportion in comparison with water and fat ^{1}H. Manipulation of different parameters affecting image acquisition allows the obtention of contrast (a difference in image intensity between two nearby regions). Images whose contrast is predominantly caused by differences in T1 of the tissues are called T1-weighted images. Similarly for T2 and ρ (ρ is the spin density or the concentration of signal-bearing spins): the images are called T2-weighted and spin density-weighted images. Other important techniques are diffusion weighted imaging (DWI), in which contrast is determined by the random microscopic motion of water protons. Functional (fMRI) is based on vasodilation detection upon brain activation due to the paramagnetic properties of haemoglobin, which produces a different T2* (a T2-related parameter) value for the water ^{1}H in the activated region.

3.3. BRAIN TUMOURS

3.3.1. Epidemiology

Tumours of the central nervous system account for less than 2% of all cancers (about 175,000 cases per year, world-wide) [18]. Incidence and

18 Stewart BW, Kleihues P, Eds. World Health Organization. World Cancer Report. 2003, Lyon, IARC Press.

mortality rates as estimated by the GLOBOCAN database [19] in 2002, for females and males are depicted in Figures 2 and 3, respectively.

19 GLOBOCAN project: http://www-depdb.iarc.fr/globocan/GLOBOframe.htm, [Accessed March 17th, 2006]

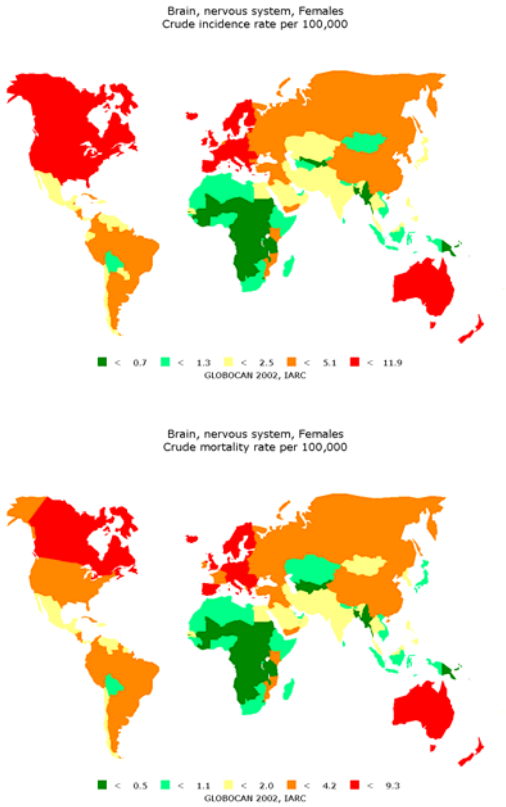

***Figure 2**: Females. Top, brain and nervous system tumours. Crude incidence rate per 100,000, females. Bottom, crude mortality rate per 100,000.*

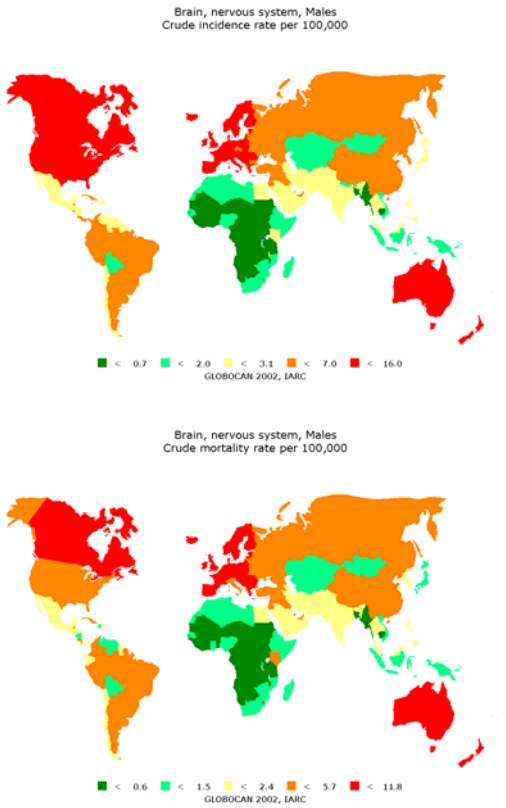

***Figure 3**: Males. Top, brain and nervous system tumours. Crude incidence rate per 100,000, males. Bottom, crude mortality rate per 100,000.*

The age distribution of tumours is bimodal, with a peak incidence in children and a second peak in adults aged 40-70 [20]. The most frequent brain tumours are those of neuroepithelial origin (60%), 28% are derived from the meninges (the brain coverings) and 7.5% are located in cranial and spinal nerves. Lymphomas and germ cell tumours account for 4% and 1% respectively. Glioblastomas – of neuroepithelial origin- are the most frequent tumour type. These tumours are highly resistant to chemotherapy and radiation and are surgically incurable, and only 3% of the patients survive more than 3 years.

3.3.2. Aetiology

The aetiology of brain tumours is largely unknown. With the exception of therapeutic irradiation, epidemiological studies have failed to detect unequivocal causative links with environmental or lifestyle factors. The effect of radiofrequency (basically by the use of mobile phones) has also been studied, but evidence is nowadays inconclusive [21]. The nervous system is frequently involved in inherited tumour syndromes, such as Neurofibromatosis, Von-Hippel Lindau Disease, tuberous sclerosis and Li-Fraumeni syndrome [22]. Simian Virus 40 (SV-40) infection by

20 Lantos Pl, Louis DN, Rosenblum MK, Kleihues P Tumours of the nervous system. In: Graham DI, Lantos PL eds, Greenfield's Neuropathology, 7th Ed, 2002, London, Arnold.
21Ahlbom A, Green A, Kheifets L, Savitz D, Swerdlow A; ICNIRP (International Commission for Non-Ionizing Radiation Protection) Standing Committee on Epidemiology. Epidemiology of health effects of radiofrequency exposure. Environ Health Perspect. 2004; 112(17): 1741-1754.
22 Kleihues P, Cavenee WK: Pathology and Genetics of Tumours of the Nervous System (World Health Organization Classification of Tumours), Ed 2. 2000, Lyon: IARCPress.

contaminated polio vaccines has also been suggested as a possible causative agent, but the issue is currently being researched [23].

3.3.3. Diagnosis

As the brain does not possess pain receptors, tumours usually grow silently until there is a mass effect and intracranial pressure is elevated, causing sometimes visual disturbance and respiratory arrest. Other times the presenting symptom is an epileptic fit or even an episode of coma. The presenting symptoms largely depend on the tumour location and the functionalities that are affected. Headache is only present when the tumour infiltrates the meninges. If the above-mentioned symptoms are present, a radiological examination should be performed, using computed tomography (CT) or magnetic resonance imaging (MRI).

A routine MR examination of the brain starts with a long TR/long TE (T2 weighted) sequence, a short TR/short TE (T1 weighted) sequence and a fluid–attenuated (FLAIR) sequence. These images are mostly performed in the transverse direction, but for specific locations other orientations can be chosen. Contrast-enhanced series are routinely performed in the transverse, coronal and sagittal plane, completed if necessary by more selective slices. Diffusion weighted imaging (DWI) is normally included in the imaging protocol nowadays, since it has important diagnostic implications, for example in the differentiation of abscesses from tumours

23 Ohgaki H, Huang H, Haltia M, Vainio H, Kleihues P. More about: cell and molecular biology of simian virus 40: implications for human infections and disease. J Natl Cancer Inst. 2000; 92(6): 495-497.

[24]. If the tumour is situated in an eloquent area, functional MR (fMRI) will better locate the lesion and define its relations to the functional areas. In order to study vessel displacement and to assess gross tumour vascularity, magnetic resonance angiography (MRA) is performed. Magnetic Resonance Spectroscopy (MRS) is performed in some clinical centres, and it is the subject of this thesis to address its clinical value in the diagnosis of brain tumours.

The diagnosis of a brain tumour with MRI includes several steps, with the last one being a tentative diagnosis of grade and type of tumour .

The first step is detection. Due to the high sensitivity of MRI to changes in water content, tumours show most of the times a hyperintense signal on T2 and FLAIR images with respect to normal brain tissue. When an exogenous contrast agent (e.g. gadolinium) is administered, detection will depend on the changes in vascularity and on the damage on the blood-brain barrier.

Then, the impact of the tumour on the brain and on the ventricles has to be evaluated. On the acute setting, the clinical situation of the patient can be better explained by the presence of hydrocephalus, midline shift and herniation than by the specific tumour type. In most cases it will be a priority to perform a ventricular drainage or to decompress a trapped temporal horn. Brain herniation can also cause secondary ischemic lesions that can determine the final prognosis of the patient. Localisation of the tumour is also important. It has to be determined whether the tumour is

24 Ebisu T, Tanaka C, Umeda M, Kitamura M, Naruse S, Higuchi T, Ueda S, Sato H. Discrimination of brain abscess from necrotic or cystic tumors by diffusion-weighted echo planar imaging. Magn Reson Imaging. 1996; 14(9): 1113-1116.

intra or extra-axial, supra or infra-tentorial and intraventricular or extra-ventricular. The tumour must be localised with respect to specific brain structures – pituitary, pineal gland or brain stem- and also with respect to functional regions and to vascular structures. Multiplanar MRI (360º) is used for this purpose, as it allows 3D reconstruction of a volume. Location with respect to specific eloquent areas is also important for treatment planning, and there are three regions of utmost importance: the Sylvian fissure (sensory and motor speech), the Rolandic fissure (sensorimotor cortex) or the calcarine fissure (visual cortex). fMRI [25] allows to visualise the functional activity of the motor, speech or visual functions. This activation can be present in the tumour itself, at its edges, or can be displaced by the mass. The exact distance between the eloquent area and the tumour will determine the operability of the tumour.

The tumour must also be located with respect to vascular structures. Magnetic resonance angiography (MRA) displays the cortical venous structure, helping in determination of the surgical approach. MRA also helps in diagnosing whether an artery is being encased, invaded or occluded. This can happen for example with the carotid artery and the middle cerebral artery in cavernous sinus lesions [26]. The next step is the determination of the extent of the lesion: whether the tumour is confined to one lobe or extends to both, whether it involves the brain stem, the basal ganglia, etc. For this, multiplanar MRI with depiction of the anatomic

25 Sunaert S, Yousry TA. Clinical applications of functional magnetic resonance imaging. Neuroimagning Clin N Am. 2001; 11(2):221-236.
26 Wilms G, Bosmans H, Marchal G, Demaerel P, Goffin J, Plets C, Baert AL. Magnetic resonance angiography of supratentorial tumours: comparison with selective digital substraction angiography. Neuroradiology. 1995; 37(1): 42-47.

relationships in the axial, coronal, and sagittal planes is mandatory. The final step in the examination of patients with a cerebral mass lesion is the differential diagnosis and the specification of tumour type and grade. For example, important questions are whether the tumour is primary or metastatic, benign or malignant, and its type: lymphomas, oligodendrogliomas, astrocytomas and meningiomas, or suspected abscess vs. tumour for example may be approached differently, varying from cyst aspiration in the case an abscess is confirmed pre-operatively, open resection in case of an astrocytic tumour, chemotherapy in case of a lymphoma, surgery plus chemotherapy for oligodendrogliomas or chemotherapy and radiotherapy for metastases.

The final diagnosis of a brain tumour is achieved with the histopathological analysis of the brain biopsy (the "gold standard" for tumour type and grade characterisation), be it stereotactic (where an external three-dimensional frame is used for location distinct areas in the brain) or from an open resection specimen. The limitations of histopathological evaluation of a biopsy piece or smear should be kept in mind, particularly with regard to glial tumours. Not only sampling can lead to an underestimation of malignancy if the biopsy is not taken from the most malignant part of the tumour [27], but also "grey zones" exist between subgroups of glial tumours [28, 29]. Moreover, stereotactic biopsy (which is

27 Burger PC, Kleihues P. Cytologic composition of the untreated glioblastoma with implications for evaluation of needle biopsies.Cancer. 1989; 63(10): 2014-2023.

28 Coons SW, Johnson PC, Scheithauer BW, Yates AJ, Pearl DK. Improving diagnostic accuracy and interobserver concordance in the classification and grading of primary gliomas. Cancer. 1997; 79(7): 1381-1393.

29 Giannini C, Scheithauer BW, Weaver AL, Burger PC, Kros JM, Mork S, Graeber MB, Bauserman S, Buckner JC, Burton J, Riepe R, Tazelaar HD, Nascimento AG, Crotty T, Keeney GL, Pernicone P, Altermatt H.

the ultimate gold standard for pre-operative diagnosis) is not exempt of significant risks of morbidity and mortality, even small. Two recent series on stereotactic biopsy that contain each a meta-analysis of 7471 [30] and 7624 cases [31] provide an estimated mortality risk range of 0.2-0.8% and an estimated morbidity (most importantly, due to haemorrhages) of 2.4-3.5% [31 , 32].

In addition to this, there is also the chance that the stereotactic biopsy yields non-diagnostic material. The same meta-analysis of the 7471 cases [30] provides an estimation of 91% diagnostic yield, which means that after stereotactic biopsy a significant 9% of patients will remain undiagnosed.

Another important issue to be considered is the operability of the tumour. In a recent prospective study in our laboratory [33], performed in collaboration with the Institut de Diagnòstic per la Imatge (IDI) and the Neurosurgery Department of the Hospital de Bellvitge (Barcelona, Spain), out of 50 patients, 10 were not operated. This represents 20% of the cases. There were several reasons: the advanced age or the physical condition of the patient, or the location of the tumour near eloquent brain areas, which posed additional risks to an operation or even a biopsy; also

---

Oligodendrogliomas: reproducibility and prognostic value of histologic diagnosis and grading. J Neuropathol Exp Neurol. 2001; 60(3): 248-262.

30 Hall WA. The safety and efficacy of stereotactic biopsy for intracranial lesions. Cancer. 1998; 82(9): 1749-1755.

31 Favre J, Taha JM, Burchiel KJ. An analysis of the respective risks of hematoma formation in 361 consecutive morphological and functional stereotactic procedures. Neurosurgery. 2002; 50(1): 48-56; discussion 56-57.

32 Field M, Witham TF, Flickinger JC, Kondziolka D, Lunsford LD.Comprehensive assessment of hemorrhage risks and outcomes after stereotactic brain biopsy. J Neurosurg. 2001; 94(4): 545-551.

33 M. Julià-Sapé, I. Coronel, C. Majós, M. Serrallonga, A. Candiota, M. Cos, J. Acebes, C. Arús. A prospective study on the added value of MRS in brain tumor diagnosis. Oral presentation. ESMRMB (European Society for Magnetic Resonance in Medicine and Biology) 2005, 22nd Annual Scientific Meeting. Magnetic Resonance Materials in Physics, Biology and Medicine (MAGMA). 2005; 18(Suppl 1): S68-S69.

the patient or the family's will was a reason, by refusing any surgical treatment in some occasions.

In all these situations, having a non-invasive tool available, which is able to correctly predict tumour type and/or grade, would constitute an important advancement towards offering better treatment to the patient.

3.3.4. Tumour types

About 120 different tumour types [22] have been described by the World Health Organization (WHO). Brain tumours can also be classified in four grades, according to their malignancy characteristics:

- WHO GRADE I: Tumours with a low proliferative potential, a frequently discrete nature, and a possibility of cure following surgical resection alone.
- WHO GRADE II Generally infiltrating tumours low in mitotic activity, but with a potential to recur. Some tumour types tend to progress to lesions with higher grades of malignancy (e.g. well-differentiated astrocytomas, oligodendrogliomas and ependymomas).
- WHO GRADE III: Histological evidence of malignancy, generally in the form of mitotic activity, clearly expressed infiltrative capabilities, and anaplasia.
- WHO GRADE IV: Mitotically-active, necrosis-prone neoplasms, generally associated with a rapid pre and postoperative evolution of the disease.

Astrocytomas constitute the majority of glial tumours, and are classified into several grades upon histopathologic examination of a biopsy sample. The most accepted classification is that of the WHO, but the St. Anne-Mayo grading criteria (Table 2) have proved to be predictive of patient survival in diffuse astrocytomas [34].

		St. Anne Mayo	
WHO grade	***WHO designation***	***Designation***	***Histological criteria***
I	Pilocytic astrocytoma		
II	Diffuse astrocytoma	Astrocytoma grade 2	One criterion, usually nuclear atypia
III	Anaplastic astrocytoma	Astrocytoma grade 3	Two criteria, usually nuclear atypia and mitotic activity
IV	Glioblastoma multiforme	Astrocytoma grade 4	Three criteria: nuclear atypia, mitoses, endothelial proliferation and/or necrosis

Table 2*: Comparison between the St. Anne-Mayo grading system for astrocytomas and the WHO grading system.*

Survival in patients afflicted by an astrocytic tumour depends on a variety of factors, and among the most important are: age and physical condition of the patient at diagnostic [35 , 36], tumour location and extent of surgical resection [37]. Pilocytic astrocytoma is the most frequent tumour type in children and locates predominantly in the cerebellum and midline structures. Its five-year survival is estimated at 85%. Some pilocytic

34 Daumas-Duport C, Scheithauer B, O'Fallon J, Kelly P. Grading of astrocytomas. A simple and reproducible method. Cancer. 1988; 62(10): 2152-2165.
35 Burger PC, Green SB. Patient age, histologic features, and length of survival in patients with glioblastoma multiforme. Cancer. 1987; 59(9): 1617-1625.
36 Sneed PK, Prados MD, McDermott MW, Larson DA, Malec MK, Lamborn KR, Davis RL, Weaver KA, Wara WM, Phillips TL, et al. Large effect of age on the survival of patients with glioblastoma treated with radiotherapy and brachytherapy boost. Neurosurgery. 1995; 36(5): 898-903; discussion 903-904.
37 Ammirati M, Vick N, Liao YL, Ciric I, Mikhael M. Effect of the extent of surgical resection on survival and quality of life in patients with supratentorial glioblastomas and anaplastic astrocytomas. Neurosurgery. 1987; 21(2): 201-206.

astrocytomas occur in the setting of neurofibromatosis type 1, particularly the optic glioma. Low-grade diffuse occur in young adults and grow slowly, diffusely infiltrating the brain and making impossible a complete resection. The five-year survival of astrocytoma II is 60%. Anaplastic astrocytomas frequently develop from low-grade astrocytomas, grow fast and progress to glioblastoma within two or three years. Glioblastomas are the most frequent and most malignant brain tumours. There are two types of glioblastomas, primary and secondary. Primary glioblastomas constitute 80% of them and are found in persons above 55 years, the expected survival being 3 months. Secondary glioblastomas develop by malignant progression from low-grade and anaplastic astrocytomas.

Oligodendroglial tumours are derived from differentiated oligodendrocytes or progenitor cells committed to oligodendroglial differentiation and can be of grades II and III, and sometimes evolve to glioblastoma multiforme.

Embryonal tumours constitute a large and important fraction of paediatric brain tumours and most of them are called medulloblastomas, which are invasive WHO grade IV tumours arising in the cerebellum, with a high tendency to cause metastases.

Meningeal tumours comprise a variety of neoplasic lesions that develop in the meninges, and most often they originate from the meningothelial cells. Meningiomas are generally benign tumours (graded into WHO grade I) attached to the dura mater, which typically manifest in adults and show a predominance for women. There are some histological subtypes that are

associated with greater likelihood of recurrence or aggressive behaviour (Table 3).

Metastatic brain tumours of the brain are originated from primary systemic neoplasms. Most of them are from carcinomas of the lung and the breast. Other frequent neoplasms that generate metastases into the brain are malignant melanoma, or renal clear cell carcinoma.

Low risk	
WHO grade	***WHO designation***
I	Meningothelial meningioma Fibrous (fibroblastic) meningioma Transitional (mixed) meningioma Psammomatous meningioma Angiomatous meningioma Microcystic meningioma Secretory meningioma Lymphoplasmacyte-rich meningioma Metaplasic meningioma
High risk	
WHO grade	***WHO designation***
II	Atypical meningioma Clear cell meningioma (intracranial) Chordoid meningioma
III	Rhabdoid meningioma Papillary meningioma Anaplastic (malignant) meningioma

Table 3*: Meningiomas grouped according to the risk of recurrence and the WHO grade.*

3.4.BRAIN TUMOUR CLASSIFICATION WITH MRS

The challenge of assigning a characteristic spectral pattern to different tumour types started to be addressed in the decade of the 90's. The first report of a spectral pattern of a brain tumour *in-vivo* was published in

1989 [38]. The spectrum of an experimentally-induced glioma in the rat was described, as well as the changes in relation to tumour growth. Two reports in 1989 [39 ,40] showed the first human spectral patterns of different brain tumour pathologies (medulloblastoma, astrocytoma and meningioma) and suggested that those differed from normal brain and also among types of tumours. In 1990 [41] the first correlation between the *in-vivo* and the *in-vitro* pattern using 11 biopsies from tumour patients was published. The idea of using metabolite ratios for comparing between cases and pathologies appears here. Ratios with respect to Creatine were compared between tumour types and it was found that the Choline/Creatine ratio differed between low-grade astrocytomas and high-grade astrocytomas, and a distinctive Alanine/Creatine ratio was found in meningiomas. The same journal published a descriptive series of 50 patients with histological verification for 49 of them in 1991 [42]. In that same year, a Danish group published another series with 17 patients [43] and again the ratios analysis was used in the comparison. The conclusion was that tumours had a relative decrease in the N-acetyl aspartate signal and in the Creatine/Phosphocreatine content with respect to normal brain

38 Remy C, Von Kienlin M, Lotito S, Francois A, Benabid AL, Decorps M. In vivo 1H NMR spectroscopy of an intracerebral glioma in the rat. Magn Reson Med. 1989; 9(3): 395-401.
39 Langkowski JH, Wieland J, Bomsdorf H, Leibfritz D, Westphal M, Offermann W, Maas R. Pre-operative localized in vivo proton spectroscopy in cerebral tumors at 4.0 Tesla--first results. Magn Reson Imaging. 1989; 7(5): 547-555.
40 Bruhn H, Frahm J, Gyngell ML, Merboldt KD, Hanicke W, Sauter R, Hamburger C. Noninvasive differentiation of tumors with use of localized H-1 MR spectroscopy in vivo: initial experience in patients with cerebral tumors. Radiology. 1989; 172(2): 541-548.
41 Gill SS, Thomas DG, Van Bruggen N, Gadian DG, Peden CJ, Bell JD, Cox IJ, Menon DK, Iles RA, Bryant DJ, et al. Proton MR spectroscopy of intracranial tumours: in vivo and in vitro studies. J Comput Assist Tomogr. 1990; 14(4): 497-504.
42 Demaerel P, Johannik K, Van Hecke P, Van Ongeval C, Verellen S, Marchal G, Wilms G, Plets C, Goffin J, Van Calenbergh F, et al. Localized 1H NMR spectroscopy in fifty cases of newly diagnosed intracranial tumors. J Comput Assist Tomogr. 1991; 15(1): 67-76.
43 Henriksen O, Wieslander S, Gjerris F, Jensen KM. In vivo 1H-spectroscopy of human intracranial tumors at 1.5 tesla. Preliminary experience at a clinical installation. Acta Radiol. 1991; 32(2): 95-99.

and that the Lactate signal was a frequent finding, especially in tumours of malignant characteristics. The origin of the Lactate signal was correlated *in-vivo* with glucose consumption in a series of 20 patients with histologically-confirmed gliomas [44]. Two techniques were combined in this study: PET (positron emission tomography) for monitoring glucose metabolism and ^{1}H-MRS for detecting the Lactate signal. It was shown that Lactate accumulation was related to glucose consumption and that this Lactate did not accumulate exactly in the areas of maximum glucose consumption but in cysts, necrotic areas and in the vicinity of the lateral ventricles. In 1992, a review by William Negendank in *NMR in Biomedicine* [45] concluded the need for improving diagnostic sensitivity of MRS of brain tumours with the use of new sequences and nuclei (^{31}P, ^{13}C and ^{1}H) and with the statistical analysis of multiple spectral features.

This early work set up the idea that first of all, MRS could be used as a tool to find diagnostic neuro-oncological markers. The results were promising as they showed that it was feasible to distinguish normal brain from brain tumour and also to differentiate among some of the most frequent tumour types (meningiomas, low-grade glial and high-grade glial tumours). Also from this period comes the use of peak ratios for comparing tumour types and also the notion pointed by William Negendank that multivariate statistical methods would be needed to distinguishing among types- as there are several characteristics (neuro-

44 Herholz K, Heindel W, Luyten PR, denHollander JA, Pietrzyk U, Voges J, Kugel H Friedmann G, Heiss WD. In vivo imaging of glucose consumption and lactate concentration in human gliomas. Ann Neurol. 1992; 31(3): 319-327.
45 Negendank W. Studies of human tumors by MRS: a review. NMR Biomed. 1992; 5(5): 303-324.

oncological markers) in each tumour type, and these characteristics are in fact variable, e.g. the Lactate signal.

From then on until the year 2000, there have been many publications using ^{1}H-MRS as a tool to find markers for different tumour types, using larger series, concentrating in specific tumour types, or in specific types of patients. It is out of the scope of this section to in-depth review all a decade's work. However, there have been important contributions towards the two following aspects:

- Multicentric studies.
- Computer-based methods for spectral classification.

Several studies reported successful automated classifications of human brain tumour spectra based on small training datasets (see also section 4) obtained at single institutions [46, 47, 48]. They contained adequate numbers of spectra from only a few groups of the more common tumours, and have usually been tested on spectra selected retrospectively from cases in which the diagnoses were known. Furthermore, they required significant operator input in the form of peak picking (i.e. performing the analysis on a few peaks in the spectrum) which weakened their objectivity and made them much less practical in routine operation. A hallmark was the article published by Preul *et al*, in *Nature Medicine* in 1996 [47], that claimed a 99% of success in classification of the five most frequent

46 Hagberg, G., Burlina, A. P., Mader, I., Roser, W., Radue, E.W., Seelig, J. In vivo proton NMR spectroscopy of human gliomas: definition of metabolic coordinates for multi-dimensional classification. Magnetic Resonance in Medicine. 1995; 34: 242-252.
47 Preul, M. C., Caramanos, Z., Collins, D.L., Villemure, J.G., Leblanc, R., Olivier, A., Pokrupa, R., Arnold, D.L. Accurate, non-invasive diagnosis of human brain tumors using proton magnetic resonance spectroscopy. Nature Medicine. 1996; 2: 323-325.
48 Usenius, J.P., Tuohimetsa, S., Vainio, P., Ala-Korpela, M., Hiltunen, Y. Kauppinen, R.A. Automated classification of human brain tumors by neural network analysis using in vivo 1H magnetic resonance spectroscopic metabolites phenotypes. Neuroreport. 1996; 7: 1597-1600.

supratentorial brain tumour types in a dataset of 105 patients obtained at their institution.

A prototype program was developed by some of the future INTERPRET partners (see also section 4), which was able to discriminate between aggressive and benign tumours with over 90% accuracy [49] using SV MR spectra obtained at long TE (135 ms) and pair wise comparisons. The system classified correctly all non-astrocytic tumours. It also combined data acquired on different instruments in different countries. However, the utility of the program was limited as it had been developed at a scientific level and was not prepared for its use in the clinical setting. Another problem was that this being a multicentric dataset, there was a degree of variability in the original histopathological diagnosis of the cases [50].

3.5. PATTERN RECOGNITION

A simple way of summarising what Pattern Recognition (PR) is could be the following paragraph by Richard Duda [51]: "The ease with which we recognize a face, understand spoken words, read handwritten characters, identify our car keys in our pocket by feel, and decide whether an apple is ripe by its smell belies the astoundingly complex processes that underlie these acts of pattern recognition. Pattern recognition – the act of taking in

49 Tate, A.R., Griffiths, J.R., Martinez-Pérez, I., Moreno, A., Barba, I., Cabanas, M.E., Watson, D., Alonso, J., Bartumeus, F., Isamat, F., Ferrer, I., Vila, F., Ferrer, E., Capdevila, A., Arús, C.. Towards a Method for Automated Classification of 1H MRS Spectra from Brain Tumors. NMR in Biomed. 1999; 11: 177-191.
50 Murphy M, Loosemore A, Ferrer I, Wesseling P, Wilkins PR, Bell BA. Neuropathological diagnostic accuracy. Br J Neurosurg. 2002; 16(5): 461-464.
51 Duda RO, Hart PE, Stork DG. Pattern classification, Second Edition. 2001. John Wiley & Sons, Inc, United States of America.

raw data and making and action based on the "category" of the pattern- has been crucial for our survival..".

PR applied to MR spectra- of brain tumours in this thesis- deals with two concepts:

- A "category" that is associated to each in-vivo brain tumour spectrum
- A mathematical process that quantifies certain features in this brain tumour spectrum and associates it to a "category".

In the INTERPRET project, for example, the "category" associated to the MR spectra was the histopathological diagnosis based on the WHO (see section 3.3.4 and reference [22]).

For an extensive explanation of the use of PR methods in MRS, a review by El-Dereedy [52] can provide useful insights. Most PR methods are derived from mathematical statistics, as in a broad sense, a PR problem can be considered as a problem of estimating density functions in a high-dimensional space and dividing this space into the regions or "categories". In INTERPRET [53] (and also in this thesis), linear discriminant analysis (LDA) has been used as PR tool. Section 3.5.1. gives an introduction to this technique.

The question of how these "categories" are established is known by "ontology" and a short summary is given in section 3.5.2.

Another important matter regarding classification is data processing. In MRS an intrinsic amount of data processing is essential in order to analyse the results of an experiment or exploration (section 3.1.3). The way in

52 el-Deredy W. Pattern recognition approaches in biomedical and clinical magnetic resonance spectroscopy: a review. NMR Biomed. 1997; 10(3): 99-124.
53 INTERPRET <http://azizu.uab.es/INTERPRET> [Accessed March 17th, 2006]

which results are quantified (fitted resonance areas or peak heights) can potentially affect performance of the PR analysis.

3.5.1. Linear discriminant analysis

Linear discriminant analysis (LDA) is used to classify cases into the values of a categorical dependent variable. It is the same idea behind multivariate analysis of variance (MANOVA), but reversed. In MANOVA, the independent variables are the groups and the dependent variables are the predictors. In LDA, the independent variables are the predictors and the dependent variables are the groups. LDA is used with two objectives:

- Descriptive. "*Discriminant analysis*" of the differences among groups.
- Predictive. "*Classification analysis*" for assigning the membership of a new observation to one of the known groups of observations.

The Bayes theorem gives the foundation to this type of approach. In the case of two groups, with distribution functions $f_1(\vec{x})$ and $f_2(\vec{x})$, the mixed density function of these two groups is:

(*Equation 4*) $$f(\vec{x}) = f_1(\vec{x})p_1 + f_2(\vec{x})p_2$$

Where p_1 and p_2 are the prior probabilities of each group, being

(*Equation 5*) $$p_1 + p_2 = 1$$

For group 1 and given an observation $\vec{x}_0$, the probability that this observation comes from group 1 is represented by the Bayes' Law:

(Equation 6) $$P(1/\vec{X}_0) = \frac{P(\vec{X}_0/1)p_1}{P(\vec{X}_0/1)p_1 + P(\vec{X}_0/2)p_2}$$

And the probability of this observation of coming from group 2 is:

(Equation 7) $$P(2/\vec{X}_0) = \frac{P(\vec{X}_0/2)p_2}{P(\vec{X}_0/1)p_1 + P(\vec{X}_0/2)p_2}$$

Which can also be expressed in terms of distribution functions:

(Equation 8) $$P(1/\vec{X}_0) = \frac{f_1(x_0)p_1}{(f_1(x_0)p_1)+(f_2(x_0)p_2)}$$

(Equation 9) $$P(2/\vec{X}_0) = \frac{f_2(x_0)p_2}{(f_1(x_0)p_1)+(f_2(x_0)p_2)}$$

The observation $\vec{x}_0$ will be assigned to the group for which we have obtained a bigger probability, *i.e*, to group 1 if:

(Equation 10) $$f_1(x_0)p_1 > f_2(x_0)p_2 \ ,$$

and to group 2 if:

(Equation 11) $$f_1(x_0)p_1 < f_2(x_0)p_2 \ .$$

In general, we assume that the function that characterises a group is a multivariate normal distribution:

(Equation 12) $$f_i(\vec{x}) = \frac{1}{(2\Pi)^{p/2}|\Sigma|}\cdot\frac{1}{2}\cdot\exp^{(-\frac{1}{2}(\vec{x}-\mu_1)\Sigma^{-1}(\vec{x}-\mu_i))}$$

Where: i=1, 2, being the groups, p the number of variables, Σ the variances-covariance's matrix, and μ the mean. We also assume that for different groups only μ changes and Σ remains constant – equal variances- or what is called the homocedasticity hypothesis. In which case for example, if the observation belongs to group 2, we can express *Equation 11* as follows:

(Equation 13) $$-\frac{1}{2}\cdot(\vec{x}_0-\vec{\mu}_2)'\cdot\Sigma\cdot(\vec{x}_0-\vec{\mu}_2)+\ln\frac{p_2}{c(2,1)} > -\frac{1}{2}\cdot(\vec{x}_0-\vec{\mu}_1)'\cdot\Sigma\cdot(\vec{x}_0-\vec{\mu}_1)+\ln\frac{p_1}{c(1,2)}$$

In fact, $(\vec{x}_0 - \vec{\mu}_2)' \cdot \Sigma \cdot (\vec{x}_0 - \vec{\mu}_2)$ is what is called the Mahalanobis distance (D^2) –a way of measuring distances- between each observation and group 2, which brings us to the geometrical interpretation of LDA: the discriminant functions attempt to maximize the separation between patterns from different classes while minimizing the separation between patterns within the same class. (Figure 4)

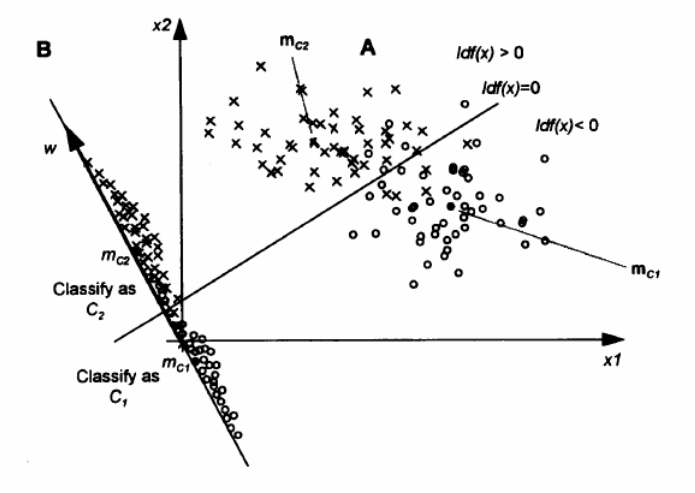

***Figure 4**: Linear discriminant functions. Part (A) finds a plane that splits the two datasets with minimum error, and the Fisher discriminant, part (B), finds a projection that maximizes the separation between the two datasets. Note hat $\boldsymbol{m}_{c1}$ and $\boldsymbol{m}_{c2}$ are vectors and m_{c1} and m_{c2} are scalars (Extracted from reference [52]).*

LDA can be extended to the *k* groups case, and in that situation there will be min(*k-1*, *p*) and *k-1* optimum directions or discriminating functions. If the groups do not have the same variance-covariance matrix, the discriminating function will be quadratic and the Σ_1, Σ_2, …, Σ_k matrices will have to be calculated, resulting in a set of quadratic discriminant functions (quadratic discriminant analysis or QDA). Non-parametric

generalisations for two or for *k* groups also exist [54]. Cost functions can be taken into account to refine the functions as well. Fundamental bibliography dealing in depth with these matters has already been given [51 , 54].

3.5.2. Ontologies

Another important matter regarding classification is how categories are set. This is known by ontology. In short, an ontology is a conceptualisation: an abstract, simplified view of the world that we wish to represent for some purpose. In a more specific language, it is a formal explicit description of concepts in a domain of discourse [55] (what are called "*classes*" or concepts), of properties of each concept describing various features and attributes of the concept (what are called "*slots*", "*roles*" or properties), and restrictions on properties (what is called "*facets*" or restrictions on properties). An ontology together with a set of individual instances of classes constitutes a knowledge base. Classes are the focus of most ontologies and describe concepts in the domain. For example, a class of tumours represents all tumours (brain, liver…) in the oncology domain. Tumour types are instances of this class. A "brain tumour" would be an instance of the class "tumours". Of course a class can have subclasses that represent concepts that are more specific. For example, we could divide the class "tumour" in subclasses according to

54 Fukunaga K. Introduction to Statistical Pattern Recognition, Second Edition. 1990. Academic Press, San Diego

55<http://www.ksl.stanford.edu/people/dlm/papers/ontology101/ontology101-noy-mcguinness.html> [Accessed March 17th, 2006]

the different organs in which they can grow (for example: "brain tumour", "breast tumour" or "liver tumour") and also subdivide the subclass "brain tumour" in "extra-axial" or "intra-axial", depending on whether it is located outside the brain tissue (in the subarachnoid space or arising from the meninges) or inside the brain tissue, respectively.

This is just an example and in general, we would be defining a brain tumour ontology when we define the concepts, the properties and the restrictions that correspond to each tumour type.

In practical terms, developing an ontology implies:

- defining classes in the ontology,
- arranging the classes in a taxonomic (subclass–superclass) hierarchy,
- defining slots (attributes) and describing allowed values for these slots,
- filling in the values for slots for instances.

Many disciplines now develop standardized ontologies that domain experts can use to share and annotate information in their fields. Examples in medicine are the SNOMED [56] or the Unified Medical Language System [57]. Specific areas may have their own ontologies, and in this respect, the INTERPRET project [58] adopted the WHO classification of brain tumours [22] in order to associate each spectrum to a definite class.

56 <http://www.snomed.org/> [Accessed March 17th, 2006]
57 Campbell KE, Oliver DE, Shortliffe EH. The Unified Medical Language System: toward a collaborative approach for solving terminologic problems. J Am Med Inform Assoc. 1998; 5(1): 12-16.
58 INTERPRET: <http://azizu.uab.es/INTERPRET> [Accessed March 17th, 2006]

3.6. MEDICAL DECISION SUPPORT SYSTEMS

The science of medical informatics started in the second half of the 1970s, and its name derives from the French term "*informatique médicale*". In medical informatics the area of research is medicine, whereas informatics constitutes its methodology. If the medical informatics research is applied, then the objective is to develop a computer system that will be used by healthcare professionals, for example in research aimed at the development of electronic medical records. If the research is more fundamental, the computer plays a role as an experimental environment for models that are developed. The objective is not to build a system, but to verify a hypothesis or to investigate the limitations of models, such as what sometimes artificial intelligence applied to medicine does [59].

Medical decision support systems (DSSs) have been defined in many ways. For example, Wyatt and Spiegelhalter define them as "active knowledge systems, which use two or more items of patient data to generate case-specific advice" [60]. In a medical DSS, medical knowledge required to reach a decision has been modelled (formally encoded). The models can be either quantitative or qualitative. Quantitative models are based in statistical methods (such as for example, LDA), and qualitative models are based on perceptions of human reasoning (decision trees or clinical algorithms). It is also frequent to combine both approaches into

59 A Knotterus, ed. The Evidence Base of Clinical Diagnosis. BMJ Books. First Ed. 2002. London, United Kingdom.
60 http://www.openclinical.org/dss.html [Accessed March 17th, 2006]

one system, and in this respect the INTERPRET SV DSS (ANNEX 1) is a combination of both philosophies: the LDA-based classifier provides a prediction by positioning all cases in a space. The user decides with the help of clinical information, visual comparison with mean spectra, and perhaps comparison with similar cases, which the diagnosis of the case is.

3.7. DATABASES

A database is a set of data elements or facts that belong to the same context, that are systematically stored for its later use. A database can be just a file with paper records. In this sense, one could consider that the first brain tumour database would be the "Cushing brain tumour registry", accrued by Dr. Harvey Cushing [61]. It is a documentation comprising more than 2000 case studies, with human whole-brain specimens, microscopic slides, hospital records, notes and photographic negatives collected from the end of the XIXth century until 1936. Another example of database could be the book by Danielsen and Ross [62], where examples of the patterns of many brain diseases are classified and described, and which could be considered as the first publicly available database of MRS patterns.

In informatics, a database is a collection of data elements stored in a computer in a systematic way, such that a computer program can consult

61 <http://www.neurosurgery.org/cybermuseum/> [Accessed March 17th, 2006]
62 Danielsen ER, Ross B. Magnetic Resonance Spectroscopy Diagnosis of Neurological Diseases. 1999. Marcel Dekker, New York, United States of America.

it to answer questions. The computer program used to manage and query a database is known as database managing system (DBMS). A DBMS is a specific software piece, serving as interface between the database and the applications used by it. The way in which data in the database is structured is known as "database model". There are several approaches to build a database model, for example:

- Hierarchical, where free-form records are linked together in a tree-structure.
- Relational, where information is structured in tables and relationships among tables are defined. The most usual DBMS language in relational databases is the structured query language (SQL) [63].

The advent of electronic communications (for example, through the Internet) allows databases to be also available through the network. A distributed database is one in which a database is linked to a distributed system and access to the data can be performed from different locations, *i.e.* different computers. For communicating between distributed databases, the so-called software agent technology can be used [64].

The commonest use of distributed databases in medicine is in electronic medical records. For example, written medical records have the purpose of documenting the care given to a patient, and thus to facilitate continuity of that care [59]. One of the major barriers for using clinical and medical tests data in different ways (epidemiological studies, quality

63 Codd EF. A relational model of data for large shared data banks. Communications of the ACM. 1970; 13(6): 377-387.
64 Brugali D. Towards Agent Oriented Application frameworks. ACM Computing Surveys 2000; 32(1): Article No. 21.

control or billing the patient, for example) is their unstructured nature, as they are normally in paper format.

There are other potential applications of distributed databases in medicine. In this respect, the INTERPRET database constitutes one of these possible applications: a distributed, hierarchical database model for the storage of clinical and MR data -SV and MV MRS, with their associated MRI data.

Another important issue in any medical database application is accuracy (completeness and correctness) or records. Special attention to this matter was devoted during INTERPRET by setting committees for clinical, histopathological, spectroscopic data validation and by following quality assurance guidelines to ensure accuracy and traceability of records.

4. SUMMARY OF THE INTERPRET PROJECT

The INTERPRET project successfully developed a computer-based decision support system to assist radiologists in diagnosing and grading brain tumours. The INTERPRET project was conceived as a multi-institutional European effort to create a DSS system that would help radiologists and other clinicians to "*interpret*" the information contained in a SV-MR spectrum of a brain tumour-like mass acquired with a 1.5 T scanner. In order to do this a large database of carefully checked heterogeneous data (MRS, MRI, histopathological and clinical data) about brain tumour patients was accrued.

Spectra from a database of ^{1}H single-voxel 1.5 T spectra of different types of brain tumours, acquired *in vivo* from 334 patients at four different centres, are clustered according to their pathology, using automated pattern recognition techniques. The results are presented as a two-dimensional scatterplot using an intuitive Graphical User Interface (GUI). Figure 5 shows the general set-up of the program. Formal quality control procedures were set up to standardise the performance of the instruments and check each spectrum, and teams of expert neuroradiologists, neurosurgeons, neurologists and neuropathologists clinically validated each case. The prototype decision support system (DSS) successfully classifies the majority of tumours in the database and helps to resolve diagnostic difficulty in borderline cases. When the prototype was tested by

radiologists and other clinicians it was favourably received. Results of the preliminary clinical analysis of the added value of using the DSS for brain tumour diagnosis with MRS showed a small, but significant improvement over MRI used alone [65]. In the comparison of individual pathologies, primitive neuroectodermal tumours or PNETs were significantly better diagnosed with the DSS than with MRI alone.

65 Lefournier V, Underwood J, Bosson J, Julià-Sapé M, van der Graaf M, Howe F, Majós C, Moreno A, Rémy C, Arús C. The added value of single-voxel proton magnetic resonance Magnetic Resonance Materials in Physics, Biology and Medicine, MAGMA. 2004; 16 (suppl 1):49.

A)

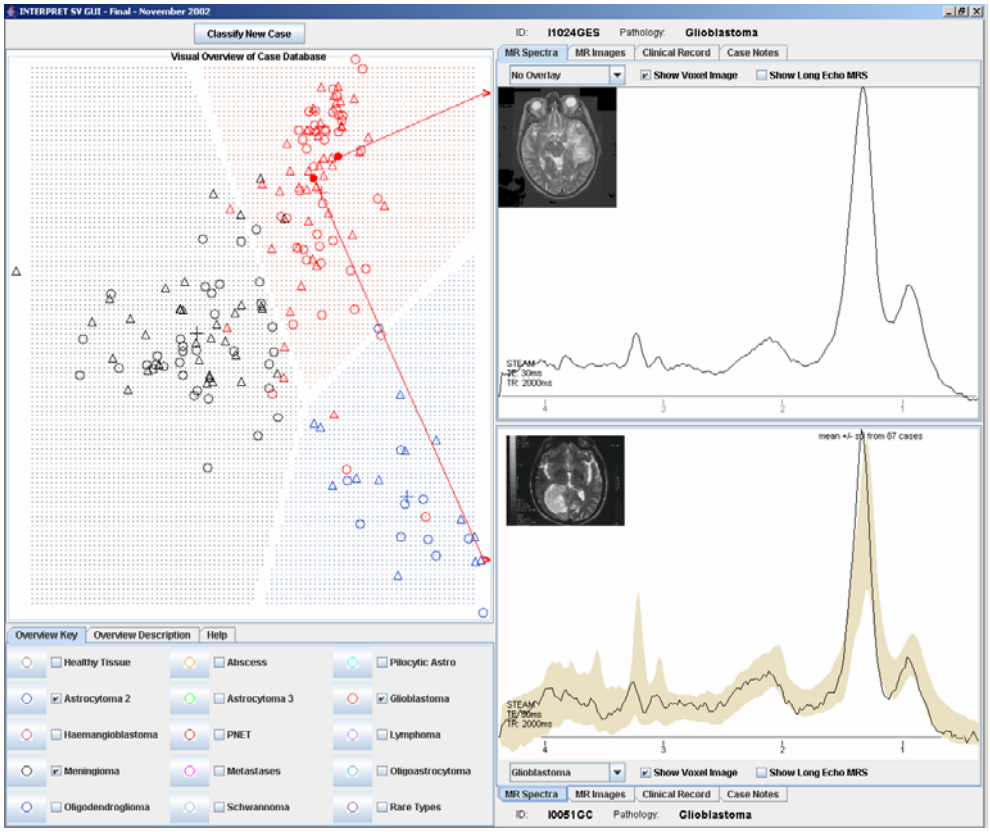
INTERPRET SV GUI - Final - November 2002
Classify New Case
Visual Overview of Case Database
ID: I1024GES Pathology: Glioblastoma
MR Spectra
MR Images
Clinical Record
Case Notes
No Overlay
Show Voxel Image
Show Long Echo MRS
STEAM
TE: 30ms
TR: 2000ms
mean +/- sd from 67 cases
Glioblastoma
Overview Key
Overview Description
Help
Healthy Tissue
Abscess
Pilocytic Astro
Astrocytoma 2
Astrocytoma 3
Glioblastoma
Haemangioblastoma
PNET
Lymphoma
Meningioma
Metastases
Oligoastrocytoma
Oligodendroglioma
Schwannoma
Rare Types
ID: I0051GC Pathology: Glioblastoma

B)

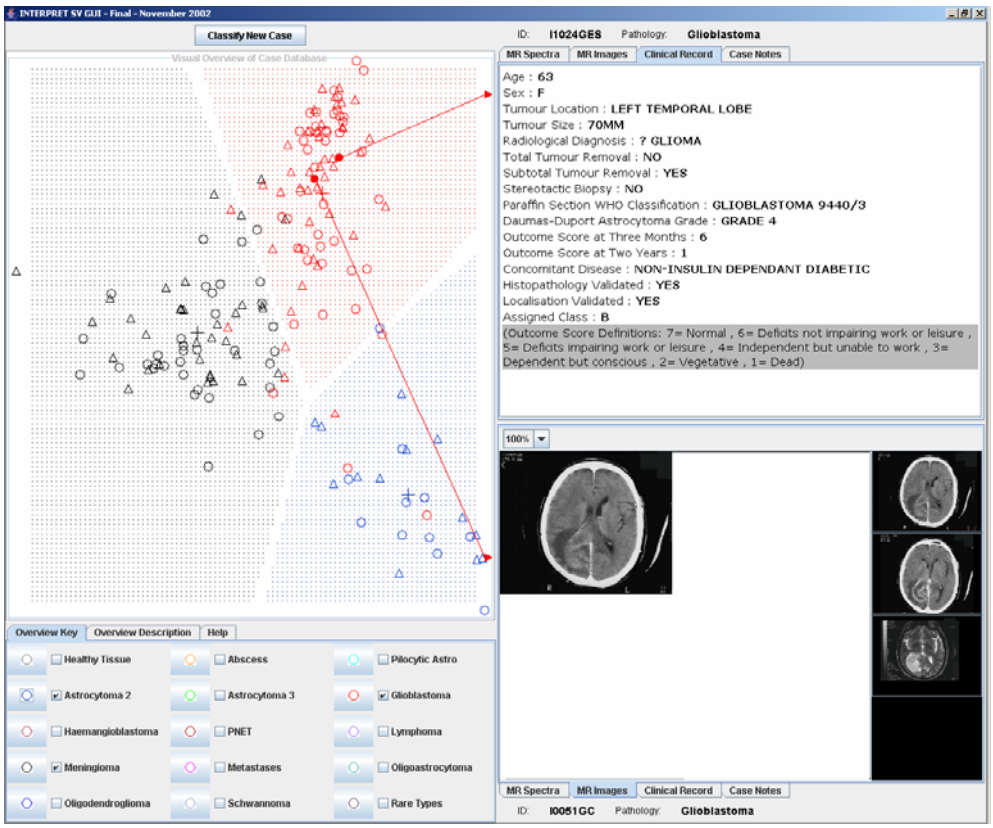
INTERPRET SV GUI - Final - November 2002
Classify New Case
Visual Overview of Case Database
ID: I1024GES Pathology: Glioblastoma
MR Spectra
MR Images
Clinical Record
Case Notes
Age : 63
Sex : F
Tumour Location : LEFT TEMPORAL LOBE
Tumour Size : 70MM
Radiological Diagnosis : ? GLIOMA
Total Tumour Removal : NO
Subtotal Tumour Removal : YES
Stereotactic Biopsy : NO
Paraffin Section WHO Classification : GLIOBLASTOMA 9440/3
Daumas-Duport Astrocytoma Grade : GRADE 4
Outcome Score at Three Months : 6
Outcome Score at Two Years : 1
Concomitant Disease : NON-INSULIN DEPENDANT DIABETIC
Histopathology Validated : YES
Localisation Validated : YES
Assigned Class : B
(Outcome Score Definitions: 7= Normal , 6= Deficits not impairing work or leisure , 5= Deficits impairing work or leisure , 4= Independent but unable to work , 3= Dependent but conscious , 2= Vegetative , 1= Dead)
100%
Overview Key
Overview Description
Help
Healthy Tissue
Abscess
Pilocytic Astro
Astrocytoma 2
Astrocytoma 3
Glioblastoma
Haemangioblastoma
PNET
Lymphoma
Meningioma
Metastases
Oligoastrocytoma
Oligodendroglioma
Schwannoma
Rare Types
ID: I0051GC Pathology: Glioblastoma

Figure 5*: A) The INTERPRET SV DSS: Left top panel: The "Overview space" provides a visual overview of the database, in which cases are represented as circles or triangles (Circles: have one or more associated MR images, triangles: have no available images). The position of each case in this space is determined by the pattern recognition algorithms with the "closeness" of any cases relating to the similarity of significant features of their spectra. The position of the mean spectrum for each pathology is marked with a cross (+). In this figure we have also chosen to "show boundaries" (boundary: line that separates two classes. Pixels which are nearly equidistant to one or more mean spectrum are not coloured, hence the white boundaries), and the zones in which we would expect to find cases from each pathology have been shaded with the same colour as the pathology (astrocytomas II: blue, glioblastomas: red, meningiomas I-II: black). When boundaries are shown in the overview, coloured pixels indicate the closest average case (cross) at any point.*

Each pathology is represented by a different colour and the user may change both the background colour and the tumour type colour. Left bottom panel: The user can select the pathologies she/he wants to see in the overview space by selecting them in the "overview key" panel. Right top panel: A glioblastoma is displayed, we can see the spectrum and a representative image of where the voxel had been placed. The position of this case in the "overview space" is indicated by the red line connecting it to the right top panel. Right bottom panel: The spectrum of another glioblastoma on which the mean and standard deviation of the glioblastoma group spectra have been superimposed (sand shade). We can see that the spectrum of this case fits into the estimated variability of this group.

B) Clicking on the "Clinical Record" tab allows the user to compare the clinical information of case I1024. Clicking on the MR Images tab allows the user to check the MR images available for case I0051.

4.1. Overall organisation of the project

The INTERPRET project involved many tasks, which were coordinated by a Project Management Team. Fundamental to the project was the accrual of a large number of ^{1}H spectra from brain lesions thought to be due to tumours. These spectra came from two sources. Many were accrued prospectively by the participating centres, using protocols and validation procedures that had been agreed upon the early stages of the project. A substantial number, however, were retrospective cases that had been scanned by the participating centres before the start of the project. In order for these retrospective spectra to be acceptable they had to have been obtained using protocols [66 , 67 , 68] compatible with those used to obtain the prospective spectra, and all the necessary clinical and histopathological data had to be validated by meeting the same requirements as those imposed on prospective cases. By including retrospective data it was possible to create a preliminary database soon after the start of the project that could be used to begin the development of the automated classification algorithms. In addition, the retrospective data substantially augmented the number of cases in the final database.

In order to "train" the system to recognise the spectral patterns of the different tumour types and to calculate the position of new spectra in the

66 Tate AR, Majos C, Moreno A, Howe FA, Griffiths JR, Arus C. Automated classification of short echo time in vivo 1H brain tumor spectra: a multicenter study. Magn Reson Med. 2003; 49(1): 29-36.
67 <http://azizu.uab.es/INTERPRET/clinical_data/clinical_data.html> [Accessed March 17th, 2006]
68 <http://azizu.uab.es/INTERPRET/clinical_data/mrs_data.html> [Accessed March 17th, 2006]

DSS overview space, classifiers based on a linear discriminant analysis (LDA) of short TE (echo time) spectra were developed [66]. Different pattern recognition approaches were used during the project, but finally LDA was shown to provide results at least as good as all other systems [69]. Furthermore, refined classifiers were incorporated at the end of the project. Lastly, a preliminary evaluation of the improvement in diagnostic accuracy when radiologists were allowed to use the DSS-based MRS data in addition to conventional MRI was carried out [65]; the improvement was quantified by Receiver Operating Characteristic (ROC) Curves analysis [70].

The project produced a prototype DSS system, which is available through the INTERPRET web page [71]. A preliminary assessment of its clinical value yielded encouragingly positive results, especially for rarer brain tumours. Unfortunately a prospective study with more patients to confirm the added value of MRS in radiological brain tumour diagnosis was not possible in the time-frame of INTERPRET.

However, the DSS was not the sole result of the project, as in order to have this system available, several other problems had to be solved first. The solutions to them constitute the other major achievements of the project and they have direct application for MRS studies of brain in other settings. These are:

- A set of consensus SV and MV 1.5 T MRS data acquisition protocols

69 Ladroue C, Howe FA, Griffiths JR, Tate AR. Independent component analysis for automated decomposition of in vivo magnetic resonance spectra. Magn Reson Med. 2003; 50(4): 697-703.
70 Obuchowski, N.A. Receiver operating characteristic curves and their use in Radiology. Radiology. 2003; 229: 3-8.
71 <http://azizu.uab.es/INTERPRET/int_Disc_Proto.shtml> [Accessed March 17th, 2006]

for instruments from several manufacturers that remains publicly available through the Internet [68]. Using these protocols, INTERPRET-compatible data can be easily obtained if a user wants to enter new data into the SV prototype described here.

- The data manipulation software (DMS), for automatically processing and calculating some quality parameters of SV MRS spectra from the most important scanner manufacturers (all GE formats up to Probe 6x, Philips format and Siemens SV Numaris and Luise postprocessed MV outputs).
- The concept of a "canonical format" used by the DMS, a first approach to a standardised MRS format. The DMS itself is used as a module plugged into the iDB so that selected information from the header is read and information is automatically incorporated into an extensive mark-up language-based database.
- The first attempt at developing standardised quality control protocols (both automated and expert-based) for checking MRS data in an objective way at the patient data level.
- Standardised clinical data validation protocols [67] for ensuring strict acceptance criteria of patient data into the study.
- The introduction of quality assurance measures under supervision of a subcontracted company for ensuring traceability and accuracy of the records [72] used to develop the systems.
- The first multi-centre, internet-available database of in-vivo MRS

72 Townsend IJ. Statistics for QA auditors of good laboratory practices and good clinical practices studies. In Good Laboratory and Clirzical Practices: Techniques for the Qualify Assurance Professiorzal, Carson PA, Dent NJ (eds). Heinemann Newnes: Oxford, 1990.

data of brain tumours [73].

- A publicly available repository of clinical history data, histopathological diagnoses and SV MR spectra of brain tumours, abscesses and adult healthy volunteers. This resource remains available to the medical community and can be used either to assist the diagnosis of brain tumour patients or for future research projects [74].
- A DSS that has undergone extensive usability testing throughout its development [75] and that has undergone a preliminary clinical assessment.

4.2. The added value of the INTERPRET DSS in clinical diagnosis

The LDA-based classifier embedded in the prototype DSS was designed for distinguishing among three aggregate-classes or tumour groups: meningiomas (WHO grades I and II), low-grade gliomas (astrocytomas, oligodendrogliomas and oligoastrocytomas WHO grade II) and high-grade malignant tumours (glioblastomas and metastases). However, the prototype is already of more general use in brain tumour diagnosis because the rest of the available cases from other pathologies and normal volunteers were also loaded into the DSS. Even though at present the

73 validated-DB: http://azizu.uab.es/INTERPRET/int_Disc_FrozenDB.shtml [Accessed March 17th, 2006]
74 eTUMOUR: http://www.etumour.net [Accessed March 17th, 2006]
75 <http://www.cogs.susx.ac.uk/users/joshuau/requirements_docs/> [Accessed March 17th, 2006]

numbers of these cases are insufficient for training discrimination algorithms and so no LDA-classifier formulas have been developed for them, in clinical practice, a new case from an unknown pathology will be automatically placed in the overview space with the LDA-classifier formulas used to classify the three main groups. The user will be able to compare a prospective case with the three aggregate-classes using for example the decision boundaries in the overview space, but will also be able to compare it with neighbouring cases from other types. Thus clinicians will be helped to "*interpret*" the SV MR spectrum of a suspicious mass before the patient undergoes surgery, so that neuroradiological assessment is enriched with additional functional and metabolic information. The patient may have a relatively uncommon brain tumour such as a grade III astrocytoma, supratentorial PNET, lymphoma, or haemangioblastoma, or a non-neoplasic mass such as an abscess. In such cases an MRS-aided radiological diagnosis may be even more helpful than for the common tumour types, e.g. meningiomas, which may often be diagnosed by MRI alone. The capability of the DSS to deliver useful information, no matter what type of tumour we input into the system, constitutes one of its strengths: not being limited to certain common classes such as "gliomas" [76], to common tissue or tumour types, *i.e.* cerebrospinal fluid, low-grade gliomas, high-grade gliomas, meningiomas,

76 McKnight TR, Noworolski SM, Vigneron DB, Nelson SJ. An automated technique for the quantitative assessment of 3D-MRSI data from patients with glioma. J Magn Reson Imaging. 2001; 13(2): 167-177.

metastasis, necrosis and healthy tissue [77], or to glial tumour grades vs. meningiomas vs. healthy tissue and cerebrospinal fluid (CSF) [78], such as in other existing DSS prototypes. In the preliminary clinical validation the INTERPRET DSS was particularly helpful with rare pathologies, such as the PNET case that was correctly classified by radiologists after using this system [65]. Although PNETs were the only individual pathology in which the improved diagnosis reached statistical significance, there was a statistically significant improvement in the overall diagnosis of all the brain tumours. However, the question still remains whether it would be possible to demonstrate the added value of using MRS with the INTERPRET DSS, or another DSS, for other individual brain tumour pathologies. The evaluation performed in INTERPRET is only a preliminary demonstration of the system's possibilities. Future studies aiming at demonstrating the added value of MRS for brain tumour diagnosis should be based on a larger series of patients, should be prospective and should also include an estimation of the performance of MRI for each individual tumour group. Furthermore, radiologists should not be limited to a few diagnoses in order to reflect day-to-day radiological practice.

77 De Edelenyi FS, Rubin C, Esteve F, Grand S, Decorps M, Lefournier V, Le Bas JF, Remy C. A new approach for analyzing proton magnetic resonance spectroscopic images of brain tumors: nosologic images. Nat Med. 2000; 6(11): 1287-1289.
78 Arjan W. Simonetti. Investigation of brain tumor classification and its reliability using chemometrics on MR spectroscopy and MR imaging data. PhD Thesis. ISBN: 90-9017814-7. Ponsen & Looijen BV Wageningen, 2004.

4.3.Limitations of the INTERPRET project and its DSS

4.3.1 Validation

There were however some inevitable limitations in the INTERPRET final SV DSS prototype of December 2002. These were essentially caused by the large workload and the coordination needed for accomplishing the main objectives of INTERPRET during the time-span of 3 years.

The most important limitation of the final INTERPRET DSS is that the data it contains do not completely satisfy the strict quality controls that were set up by the project. The final version of November-December 2002 contains several erroneous data, for example:

- There are short TE spectra that do not correspond to what they should, as it is described in Figure 6 .
- Some clinical information is not consistent. For example, case I0423. The final DSS gives the following information: "Subtotal tumour removal = No" and "Total tumour removal = No" and "Stereotactic Biopsy = NO". The INTERPRET database (the iDB) gives the following information: "Subtotal tumour removal = Yes" and "Total tumour removal = No" and "Stereotactic Biopsy = NO"
- Cases that had been entered in the DSS version prior to being entered in the database and thus have an independent coding system (some

normal volunteers from one of the contributing centres, CDP: N1200GC, N1218GC, N1564GC, N1565GC and NI967).

- Not all cases in the DSS had all the information available entered in the prototype. Namely, characteristic images of the case: T1 and T2-weighted and the image displaying where the voxel had been placed. For this reason, a part of the cases are symbolised with circles (those with images available) while the other are symbolised with triangles in the overview space.

The source of these errors was that most tasks in INTERPRET had had to be performed in parallel:

- Database development, being itself a research project and meeting the requirements of being functional for data upload and on-line quality control early in the project's development, while solving user requests for incorporation of additional functionalities.
- Data collection and upload to the database.
- The clinical validation committee, validating retrospective and prospective data, from the clinical and histopathological point of view- also in parallel, until three months before the project's end, as prospective data were acquired until that time.
- Pattern Recognition (PR): using the available datasets at different time-frames for constantly refining the classifier systems.
- DSS development and testing, for usability and at the same time keeping up-to-date versions of the latter validated dataset which was continuously growing by progress in data accrual and validation.

In order to have a DSS that contained fully reliable data, some additional work needed be performed:

1) Purging the data in the INTERPRET final SV DSS that did not fulfil all quality requirements set up by the project. This means that that each case should have at least one single voxel (SV) short-echo (20-32 ms) 1.5 T spectrum acquired from a nodular region of the tumour, that the voxel had been positioned in the same region where subsequent biopsy was obtained, that the short echo spectrum had not been discarded because of acquisition artefacts or other reasons, and that a histopathological diagnosis was agreed among a committee of expert neuropathologists. When the spectra were obtained from normal volunteers or abscesses and clinically-proven metastases, biopsy should not be needed.
2) Keep the validated data together in one place, *i.e.* into a database.
3) Retrain the classifier.
4) Migrate the checked data into a new version of the DSS.

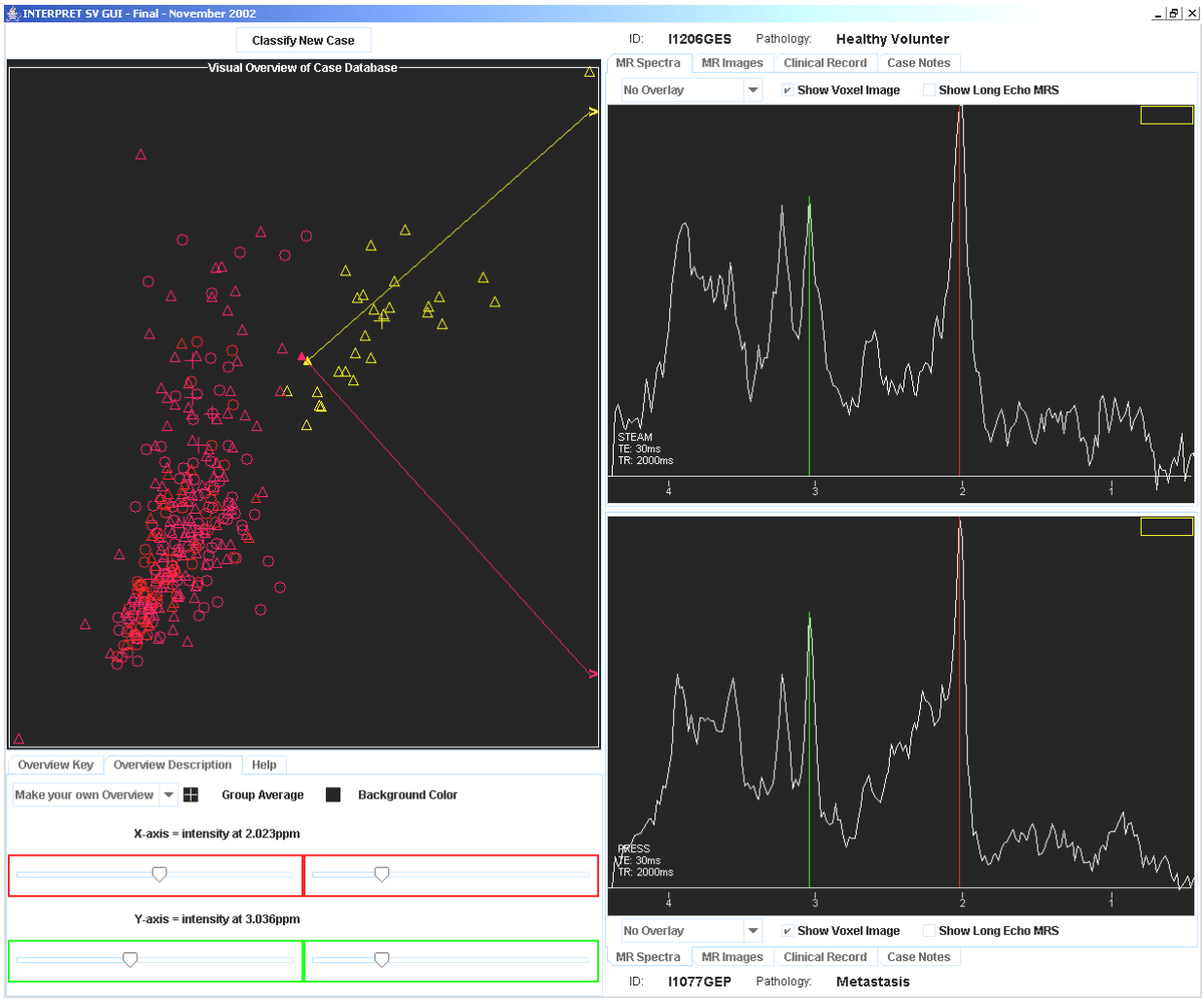

***Figure 6**: Personalised overview space: peak heights scatterplot of NAA vs. creatine. X axis: intensity at 2.023 ppm, Y axis: intensity at 3.036 ppm. Normal brain spectra are grey symbols while the other colours are tumours and abscesses. Top right panel: case I1206; bottom right panel:case I1077, a metastasis. Case I1206 (example of a normal volunteer) shows an NAA peak that is less than double the intensity of the creatine and choline signals (as it would be expected from the mean spectra).Spectroscopic quality parameters were acceptable but borderline: SNR= 37.00 (acceptance threshold> 10) and WBW= 7.40 Hz (acceptance threshold <8 Hz), and the spectrum had been discarded by one out of three spectroscopists because of the poor SNR and WBW values for a normal control. This is an example of borderline case that can receive a conflicting interpretation ("is this a tumour?") due to impaired instrumental quality. Case I1077 was a metastasis that was discarded in the final round of quality checks after the end of the project because of voxel not being entirely placed in the tumoural zone, and thus this case was not included in the validated-DB and in further post-INTERPRET versions of the DSS ([79]).*

79 <http://azizu.uab.es/INTERPRET/int_Disc_Proto.shtml> [Accessed March 17th, 2006]

4.3.2. Short vs. long TE in brain tumour classification

Despite the large amount of data collected for INTERPRET, with protocols that required one short TE and one long TE measurement, only short TE was used for developing the PR classifier embedded in the DSS. However, the system could potentially have used the long TE spectra that had been collected.

At long TE (TE > 45 ms) a reduced number of metabolites is observed as compared to short TE altough long TE has less baseline distortion, yielding a spectrum that is easier to process, analyse, and interpret. At approximately 136 ms, Alanine and Lactate doublets are inverted because of J-coupling, making it easier to differentiate these resonances from lipids and macromolecules. At short TE, more resonances are visible because the signal intensity from compounds with strong J-modulation (spin-spin coupling) may be lost at long TE apart from resonances with a short T_2. Accordingly a short TE is required for better evaluation of some particular compounds (e.g. lipids, Myo-Inositol, Glutamine and Glutamate). Moreover, TE affects not only the appearance of the peaks but also their intensity, depending on the differing T2 relaxation times of metabolites and macromolecules [80 , 81 , 82 , 83, 84]. A preliminary analysis during the course of the INTERPRET project showed that distinguishing between

80 Kaminogo M, Ishimaru H, Morikawa M, Ochi M, Ushijima R, Tani M, Matsuo Y, Kawakubo J, Shibata S. Diagnostic potential of short echo time MR spectroscopy of gliomas with single-voxel and point-resolved spatially localised proton spectroscopy of brain. Neuroradiology. 2001; 43(5): 353-363.
81 Castillo M, Kwock L, Mukherji SK. Clinical applications of proton MR spectroscopy. AJNR Am J Neuroradiol. 1996; 17(1): 1-15.
82 Danielsen ER, Ross B. Basic physics of MRS. In: Danielsen ER, Ross B, ed. Magnetic Resonance Spectroscopy Diagnosis of Neurological Diseases. New York: Marcel Dekker, Inc; 1999: 5-22.
83 Kwock L. Localized MR spectroscopy: basic principles. Neuroimaging Clin N Am. 1998;8(4):713-731.
84 Candiota AP, Majos C, Bassols A, Cabanas ME, Acebes JJ, Quintero MR, Arus C. Assignment of the 2.03 ppm resonance in in vivo 1H MRS of human brain tumour cystic fluid: contribution of macromolecules. MAGMA. 2004;17(1):36-46.

metastases and glioblastomas was more difficult at 136 ms, and that an LDA using 3.72, 3.04, 2.31, 2.14, 1.51 and 1.20 ppm peak heights as input features and meningioma, high-grade malignant and low-grade glioma as groups, produced fewer correct classifications than for the short TE spectra. In this instance, a slightly lower percentage of cases of the previously-defined groups of interest from an independent test set were correctly classified (83%) than when short TE data were used (89%). A systematic test of which echo time was better for classifying tumour types was finally performed, as long and short TE datasets were not completely paired, i.e. although most cases had at least one short and one long TE spectrum, a proportion of cases had only either short or long TE spectra, and in other cases while the two TEs were available one of the two spectra was discarded because of instrumental reasons.

An additional problem that could not be solved during INTERPRET was that the Data Manipulation Software (DMS) for automated processing was not producing perfect-quality spectra in some instances. In these cases, the Klose algorithm [85] for Eddy Current correction was not sufficient for correcting the phase and some further manual (by the spectroscopist) phasing was needed, especially in some of the Philips spectra of the database that were acquired at one of the contributing centres before a software fix was performed by the manufacturer. (Figure 7).

There were also slight misalignments in some of the automatically processed spectra (frequency offset was not entirely corrected) (Figure 8),

85 Klose U. In vivo proton spectroscopy in presence of eddy currents. Magn Reson Med. 1990; 14(1): 26-30.

which could hamper the use for classification of automatically-processed long TE spectra with the DMS in its final INTERPRET version.

For testing which TE is better (short or long), a completely paired dataset of both short and long TE spectra acquired from the same series of patients was needed. Moreover, the processed spectra of that dataset should be free of any artefact such as misalignment or imperfect phasing.

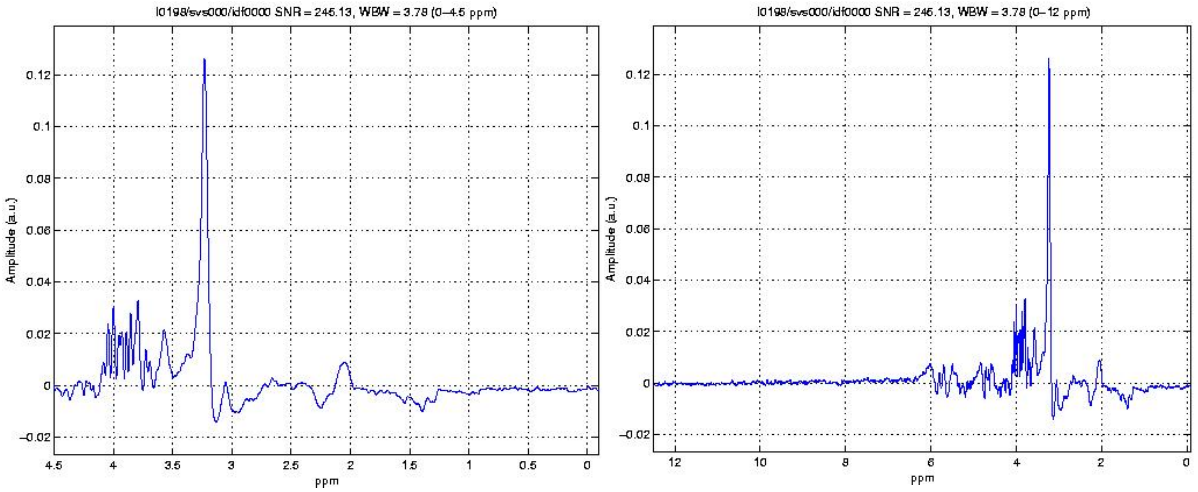

Figure 7*: Case I0198 in the iDB. A Philips PRESS 136 ms TE spectrum. Top: 0-4.5 ppm. Bottom: 0-12 ppm. SNR: Signal to noise ratio. WBW: water bandwidth at half height. For details about these definitions check ANNEX 1. This spectrum was labelled as having a phase problem by two out of three expert spectroscopists. Note that the top of the Creatine peak at 3.03 ppm has an amplitude value in a.u of 0.*

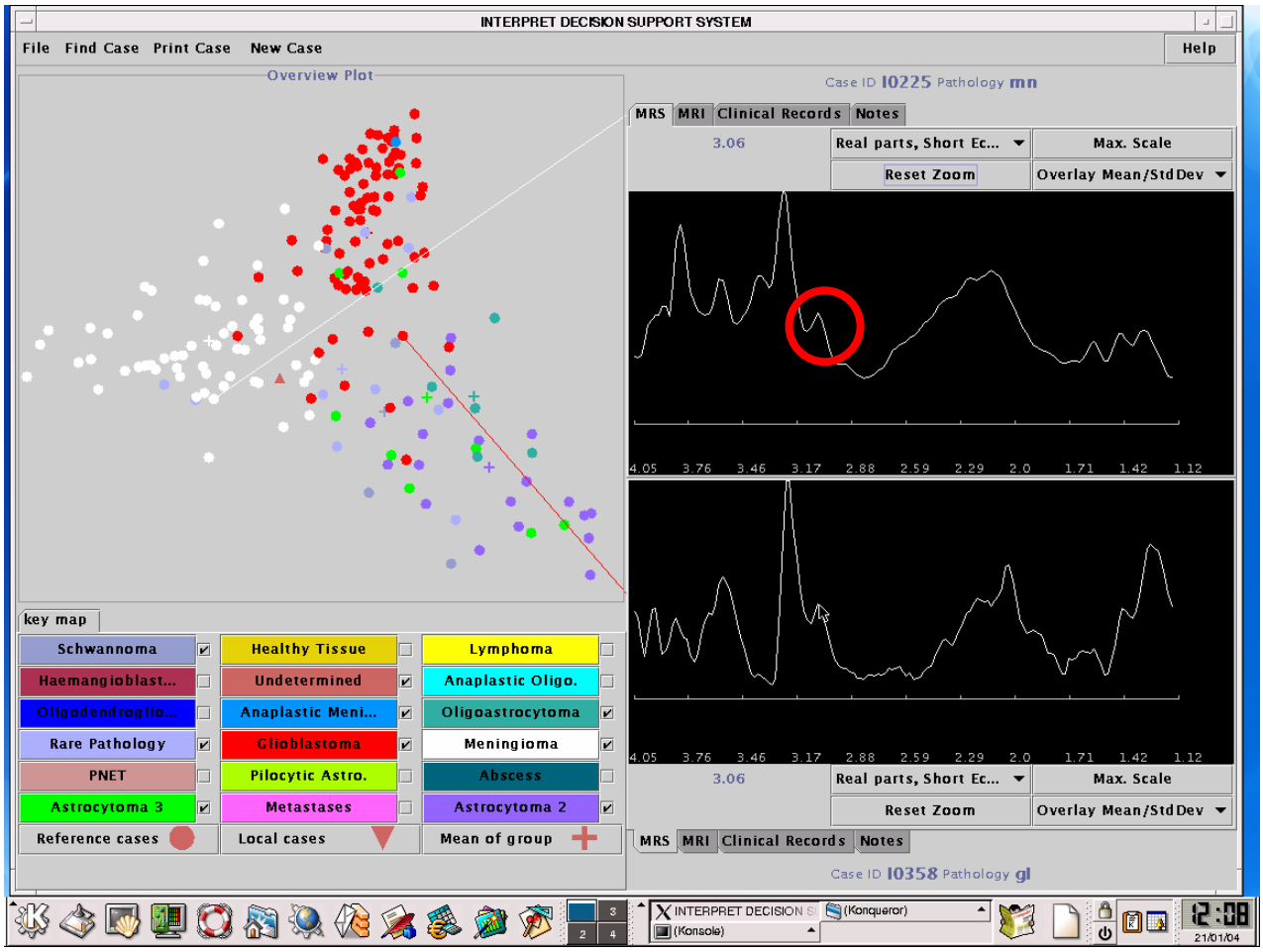

***Figure 8**: Two cases in the industrial version of the INTERPRET prototype. It can observed that the top of the creatine peak is labelled at 3.06 ppm (red circle), whereas the expected value would be 3.03 ppm.*

4.3.3. Data sparsity and ontologies

It soon became apparent in INTERPRET that there would not be enough cases available for performing a PR analysis of each of the approximately 100 tumour types and tumour-like lesions of the WHO classification of brain tumours.

The analysis of high-dimensional (*e.g.* MR spectra, microarrays) is characterised by the so-called "curse of dimensionality" and the "curse of

data sparsity" [86]. The number of features characterizing the data (MRS data) exceed by far the number of samples available for each type to be analysed.

On the other hand, it is not advisable to use a high number of features and a low number of samples in statistical PR, as it is possible that the model that we obtain is "overfitted" to the small population we study. The model would work in our dataset but when a new, different, dataset is tested against our model it would fail. Solving the "small sample size" [54] problem for LDA (and other statistical techniques as well) is currently an active topic in statistical research.

The following example will illustrate the issue of data sparsity and high dimensionality: There are brain tumour types with a low prevalence in the general population: *e.g.* craniopharyngiomas, with an incidence of 1.3 cases per 1,000,000 persons per year [87]. Short TE MR spectra at 1.5 T can potentially have around 20 features (metabolite peaks) if fitted – integrated- peak areas are taken as input features (Table 1), or even a number ranging from 512 to 2048 (depending on the scanner manufacturer) if the whole spectral vector is taken as input for our PR analysis.

From a practical point of view, if a sample-to-feature ratio of 3:1 was used for training the PR algorithm, and only 2 features for classifying craniopharyngiomas were used, we would need to gather all available

86 Somorjai RL, Dolenko B, Baumgartner R. Class prediction and discovery using gene microarray and proteomics mass spectroscopy data: curses, caveats, cautions. Bioinformatics. 2003; 19(12): 1484-1491.
87 Bunin GR, Surawicz TS, Witman PA, Preston-Martin S, Davis F, Bruner JM. The descriptive epidemiology of craniopharyngioma. J Neurosurg. 1998; 89(4):547-551.

cases in a population of about 4.5 million people (the approximate population of Norway in July 2005 [88]) for potentially having 6 cases available for our analysis. The INTERPRET full database that contains all the data accrued during the project contains spectra for 774 cases. Only one case in the database is a craniopharyngioma.

For these two reasons, data sparsity and high dimensionality, PR in INTERPRET was performed by considering some types of tumours as a single entity. That was what was called "pathology groupings" [89]. Data that belonged to tumour types that had a similar clinical behaviour were joined into a single group for performing PR. For example, all astrocytomas of WHO grade II were joined in a single group of "Low-grade astrocytomas". Even in that situation, the low number of cases in some classes and the non-separability of other classes caused that additional groupings –broader types- were considered in the final analysis (Table 4). "Low-grade astrocytomas" were grouped with "low-grade oligodendrogliomas" and "low-grade oligoastrocytomas" to form a class of "low-grade glial tumours".

In this respect, the groupings used in PR during INTERPRET may constitute a very simple ontology with three classes, where the tumours with histopathological diagnoses that belonged to each class could be considered as instances of the classes.

88 <http://www.cia.gov/cia/publications/factbook/rankorder/2119rank.html> [Accessed March 17th, 2006]
89 <http://azizu.uab.es/INTERPRET/DocDir/HCTCNS_4.pdf> [Accessed March 17th, 2006]

Group	Histopathological diagnoses
Low-grade glial	Diffuse astrocytoma 9400/3 Fibrillary astrocytoma 9420/3 Protoplasmic astrocytoma 9410/3 Gemistocytic astrocytoma 9411/3 Pleomorphic xanthoastrocytoma 9424/3 Subependymal giant cell astrocytoma (Tuberous sclerosis) 9384/1 Oligo-astrocytoma 9382/3 Oligodendroglioma 9450/3
Meningioma	Meningioma 9530/0 Meningothelial meningioma 9531/0 Fibrous (fibroblastic) meningioma 9532/0 Transitional (mixed) meningioma 9537/0 Psammomatous meningioma 9533/0 Angiomatous meningioma 9534/0 Microcystic meningioma 9530/0 Secretory meningioma 9530/0 Lymphoplasmacyte-rich meningioma 9530/0 Metaplasic meningioma 9530/0 Clear cell meningioma 9538/1 Chordoid meningioma 9538/1 Atypical meningioma 9539/1
Aggressive	Glioblastoma 9440/3 Giant cell glioblastoma 9441/3 Gliosarcoma 9442/3 Metastatic Tumours 8000/6

***Table 4**: Pathology groupings considered for the INTERPRET DSS PR analysis.*

However, not all tumour cases in the database were represented in this ontology and thus not all types and individual cases were used in the PR analysis (lymphomas, medulloblastomas, etc), even if it might be clinically important to be able to distinguish them by MRS.

On the other hand, there are as well classes that are not easily separable by MRS, such as glioblastomas and metastases [17].

In this respect it has still to be shown whether an histopathology-based ontology would be applicable when dealing with MRS or with MRI data.

4.3.4. Does MRS really help brain tumour diagnosis?

No significant differences between MRI and MRS-assisted diagnosis of tumour type during the clinical evaluation phase of INTERPRET were found for individual type comparisons, except in medulloblastomas. For some pathologies, the diagnostic performance measured as the Area Under the Curve (AUC) of Receiver Operating Characteristic (ROC) curves plotted with the test results was close to the ideal value of 1. Meningiomas, with 20 measurements, gave an AUC for MRI of 0.96 ±0.03, and an AUC after using the DSS of 0.97 ± 0.03. In this situation, it would be extremely difficult to observe significant differences between the two situations, and perhaps a much larger dataset would be needed to demonstrate that there are significant differences between the uses of both techniques. In other pathologies the AUC was in the range of a random test, for example in medulloblastomas (n = 6) when MRI was used (AUC =0.50 ± 0.12). After using the DSS, the AUC was significantly increased to a value of 0.83 ± 0.12. Whether MRS can be of help precisely in the tumour types that are more difficult to distinguish with MRI alone still remains to be investigated in detail.

In order to demonstrate that the MRS technique is of clinical value, it must be shown that it significantly helps both tumour typing and grading, with a larger dataset, and in a prospective form. The dataset used in the preliminary clinical evaluation of INTERPRET comprised 16 cases and the large n for some types corresponds to the number of observations that

were performed by different clinicians on the same case. Nevertheless, being a small dataset there is the risk that it was not sufficiently representative of the general brain tumour population, *i.e*. the n=6 of the medulloblastoma comparison comes from a single case, which might have been a specially difficult one.

And finally, if MRI is to be used as a reference technique for comparing with MRS, its diagnostic performance values must also be carefully estimated with the help of a larger dataset.

5. OBJECTIVE

As a result, this thesis addresses the following questions:

A)-Is it possible to have a prototypical "INTERPRET dataset" that satisfies all the quality requirements set up by the project?

B)-Which echo time is more informative for brain tumour classification?

C)-In which tumour types it will be more useful to have a good discriminatory power using MRS?

6. ARTICLES

6.1. ARTICLE 1

A multi-centre, web-accessible and quality control-checked database of in vivo MR spectra of brain tumour patients.

Julià-Sapé M, *Acosta D, Mier M, Arús C, Watson D; INTERPRET consortium*

MAGMA. 2006 Feb;19(1):22-33. Epub 2006 Feb 14

http://www.springerlink.com/content/elq1x6776h8p261k/

6.2. ARTICLE 2

Brain tumour classification by proton MR spectroscopy: Comparison of diagnostic accuracy at short and long TE

Majós C, ***Julià-Sapé M****, Alonso J, Serrallonga M, Aguilera C, Acebes JJ, Arús C, Gili J*

AJNR Am J Neuroradiol. 2004 Nov-Dec;25(10):1696-704

http://www.ajnr.org/cgi/content/full/25/10/1696

6.3. ARTICLE 3

Comparison between neuroimaging classifications and histopathological diagnoses using an international multicenter brain tumor magnetic resonance imaging database.

Julià-Sapé M, *Acosta D, Majós C, Moreno-Torres A, Wesseling P, Acebes JJ, Griffiths JR, Arús C*

J Neurosurg. 2006 Jul;105(1):6-14

http://www.thejns-net.org/jns/issues/v105n1/pdf/n1050006.pdf

7. GENERAL DISCUSSION

7.1. Validation

As it has been stated in Section 4, in order to have a DSS available that has been "trained" with completely reliable data, additional work was needed, for which there was not time enough during INTERPRET:

1. Purging the data in the final INTERPRET SV DSS that did not fulfil all quality control requirements that had been set up.
2. Putting data together in the same place: having a database with all entries carefully checked.
3. Retraining the classifier.
4. Uploading the checked data into a new version of the INTERPRET SV DSS.

Steps 1 and 2 are the subject of ARTICLE 1 of this thesis. Accomplishment of steps 3 and 4 has already been achieved by September 2005 (Post-INTERPRET SV prototype versions 1.1 and 1.2, accessible through the INTERPRET web page [71]). These prototypes are not part of this thesis although its author has collaborated in their development [90, 91]. The importance of covering steps 1 and 2 lies in that a database with quality

90 Mercadal G, Julià-Sapé M, Coronel I, Aguilera C, Underwood J, Arús C. Version 1.2 of an interactive decision-support system for brain tumour diagnosis using single voxel MRS data. Magnetic Resonance Materials in Physics, Biology and Medicine MAGMA. 2005; 18(Suppl 1): S218-S219

91 http://rsna2005.rsna.org/rsna2005/V2005/conference/event_display.cfm?em_id=4407534 [Accessed March 17th, 2006]

control-checked data is made available, making it possible to develop post-INTERPRET prototype versions. These have the following new features with respect to the final INTERPRET version:

- All SV short TE spectra from tumour cases have been acquired from a nodular region of a tumour, avoiding cystic, oedematous regions that have a different spectral pattern.
- Clinical information is correct.
- All cases have an INTERPRET coding, being traceable to the validated-DB and the original source of data in the clinical centre.
- All cases in the DSS have all the information available in the database.

Other improvements have also been incorporated into the post-INTERPRET versions of the SV DSS, through developments in the DMS software, such as alignment and phase adjustment. This will not be discussed here and details can be found at the prototype download pages [71].

The validated-DB constitutes a European resource for clinicians worldwide using MRS to help in non-invasive diagnosis of brain tumours. It is accessible upon signature of a disclaimer form and the evaluation of the request by the consortium. Instructions can be found at:

http://azizu.uab.es/INTERPRET/int_Disc_FrozenDB.shtml

The database in its current state can be used as a flexible, on-line resource documenting system of clinical brain tumour cases, allowing comparison with cases obtained at other clinical institutions in compatible conditions, in a similar way as using a book [62].

This database exists as well in a replicate version that is currently being used by the VIth Framework EU eTumour project [92] as "preliminary eTumour database".

http://azizu.uab.es/etumourDB/

The difference with the validated-DB lies in that the "preliminary eTumour database" allows authorised users to download raw data for their analysis, whereas the validated-DB only allows viewing the data. The preliminary eTumour-DB has been made available since the beginning of 2004 to the eTumour consortium and serves to develop preliminary classifiers for the eTumour project which should be improved with respect to INTERPRET [66, 93, 94, 95] due to the superior quality of the data it contains now. This database is to be expanded with recruitment of new patients and acquisition of more data types (HR-MAS and microarrays) in the context of the eTumour project. The eTumour database is currently benefiting from the experience gained in INTERPRET, with regard to both its design and contents.

92 http://www.etumour.net [Accessed March 17th, 2006]
93 Devos A, Lukas L, Suykens JA, Vanhamme L, Tate AR, Howe FA, Majos C, Moreno-Torres A, van der Graaf M, Arus C, Van Huffel S. Classification of brain tumours using short echo time 1H MR spectra. J Magn Reson. 2004; 170(1): 164-175.
94 Devos A, Simonetti AW, van der Graaf M, Lukas L, Suykens JA, Vanhamme L, Buydens LM, Heerschap A, Van Huffel S. The use of multivariate MR imaging intensities versus metabolic data from MR spectroscopic imaging for brain tumour classification. J Magn Reson. 2005; 173(2): 218-228.
95 Ladroue C, Howe FA, Griffiths JR, Tate AR. Independent component analysis for automated decomposition of in vivo magnetic resonance spectra. Magn Reson Med. 2003; 50(4): 697-703.

7.2.Short vs. long TE in brain tumour classification

In the study presented in ARTICLE 2, areas were used as input features instead of peak heights. In this way, possible variations due to misalignments and incorrect phasing on automatically processed spectra were avoided: spectra were manually processed and corrected for phase, baseline and referencing. On the other hand, the use of areas decreased the number of input features for the classifier. And third, at the time of performing the study in Article 2 (January-May 2003), the automated routines of the DMS had not yet been adapted for their easy use.

This study provides evidence in favour of classifier combination for improving brain tumour classification with MRS. We found that if the classifier gives the same answer at both echo times, the chances that this is the correct answer are higher. This result is of importance especially in studies in which data from several echo times may be acquired.

Besides, the notion of using several classifier systems for the same case suggests that in clinical practice, using the "definitive" classifier at the "definitive acquisition conditions" would not be advisable. The more information the better, which in fact comes from common sense. The biochemical information given by coupled spin systems such as the inverted Lactate or Alanine peaks at long TE, the different visibility of

mobile lipids with varying TE or the modulation of some resonances such as Glycine and Myo-Inositol should not be discarded as input for PR analyses. In this respect votation schemes [96] – among other approaches, - could help to fully exploit the information contained in data acquired at different TEs.

In the prospective study mentioned in the introduction [33], we used the classification results of the short TE area classifier, of the long TE area classifier, the INTERPRET DSS and the expert spectroscopist knowledge in a combined way – with the use of a strict decision protocol- for giving an MRS-based diagnosis. One of the results of the study was that using this approach, MRS devoid of any further information (age, sex, tumour location) was as good as MRI in the orientation of brain tumours. More details of the study will be given elsewhere.

One the other hand, a detailed study of the use of areas and peak heights at the different echo times was still needed. At the time of presenting this thesis a study performed in this respect is already finished [97 , 98], in which the author of this thesis has collaborated, but its results will not be presented here.

96 Minguillón J, Julià-Sapé M, Mercadal G, Moreno A, Arús C. Bagging decision trees for studying the discriminative power. Magnetic Resonance Materials in Physics, Biology and Medicine MAGMA. 2004;16 (suppl 1): 48-49

97 I. Coronel, M. Julià-Sapé, C. Majós, G. Mercadal, S. Castañer, J. Acebes, C. Arús. Comparison of brain tumour classification performance with different echo times and feature extraction methods. Magnetic Resonance Materials in Physics, Biology and Medicine (MAGMA) 2005; 18(Suppl 1): S192-S193.

98 Coronel I, Serrallonga M, Julià-Sapé MM, Cos M, Candiota AP, Castañer S, Acebes JJ, Majós C, Arús C . A prospective study on the added value of in vivo MRS in brain tumour diagnosis Neuroradiology. 2005; 47(Supplement 1): S78.

7.3. Data sparsity and ontologies

The ontology that was developed in Article 3 (Figure 9) can aid in MRS research by increasing the number of available cases for the analysis. Even in cases that belong to very uncommon brain tumour types it will be possible to assign them to a higher-order entity (super-class, meta-class), and therefore to analyse it in some way. The validated-DB contains only two cases with the diagnosis "anaplastic oligoastrocytoma". It will always be possible to search for patterns in the MRS data of these cases by taking into account the different information levels available in the WHO histopathological diagnosis that characterises them:

- it has the HIGH grade attribute as it is a high-grade (WHO grade III) tumour,
- it belongs to the glial super-class, so it can be joined with other glial tumours,
- it belongs to the neuroepithelial meta-class of tumours, so it can be joined with other neuroepithelial tumours.

In this way, it can be investigated at which level (meta-class, super-class or class) the different types of tumours can be separated using MR-based techniques (for example, MRS).

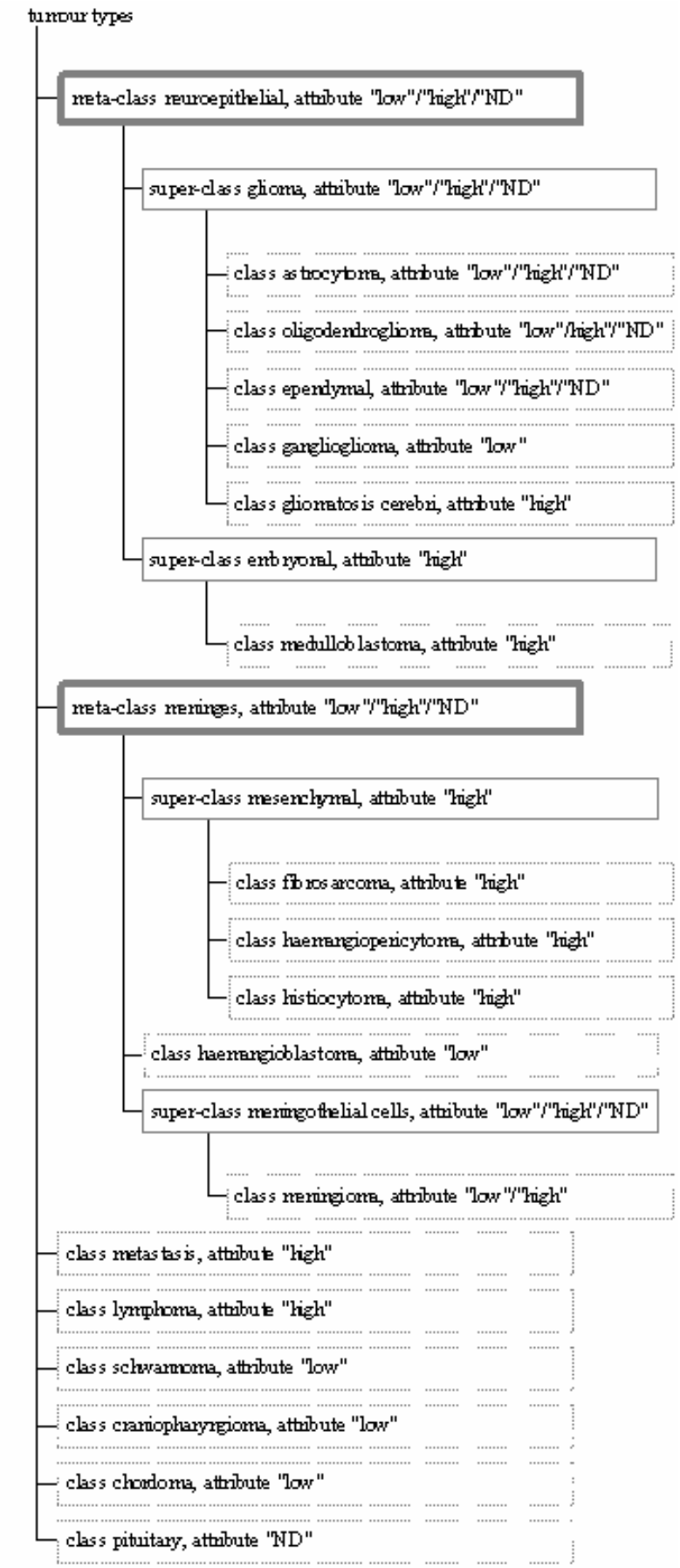

***Figure 9**: Hyerarchical tree representing the ontology defined for this study.*

7.4.Does MRS really help in brain tumour diagnosis?

Article 3 does not resolve the question of whether MRS is or is not of help in brain tumour diagnosis, but contains several relevant new considerations towards the achievement of this goal:

- In contrast to previous studies [46 , 47 , 48 , 49], which considered all cases from all tumour types together in a pool of right/wrong diagnoses, this work starts from the premise that there might be tumour types that are easier to differentiate than others. In this respect, an individual analysis of the different types was needed and an ontology was developed for this purpose. A novelty has also been to consider type and grade of the tumour as separate concepts in order to characterise test performance even more precisely.
- More adequate measures than in previously referenced studies [46 , 47 , 48 , 49] have been calculated. Previous studies had used accuracy (ratio between the correctly classified cases and the total number of cases). In this work, Sensitivity, Specificity, Positive Predictive Value and Negative Predictive Value have been used. These are commonly accepted measures for evaluation the performance of a clinical test [59 , 99].

99 Altman DG, Machin D, Bryant TN, Gardner MJ. Statistics with Confidence, Ed 2. 2001. British Medical Journal Books, Bristol, United Kingdom.

- Most importantly, this work gives the "ground values" for any other MR-based technique (such as for example, MRS) to be tested against MRI in the diagnosis of brain tumours. This introduces a Bayesian perspective in the assessment of the MRS technique for brain tumour diagnosis [100], *i.e.* it gives the post-test values of MRI for the different types of brain tumour types. When several tests must be compared (MRI and MRS), Bayes theorem can be applied sequentially by using the posterior probability of one test as the prior probability for the next test. Thus, the values obtained in Article 3 can be used as pre-test values for the future assessment of the diagnostic value of the application of MRS after MRI.

But, what are pre and post-test probabilities? The pre-test (prior) probability of a disease is the probability of the presence of this disease conditioned on the available information prior to performing the test under consideration. The post-test (posterior) probability of disease is the probability of the presence of the target disease conditional on the pre-test information and the test results. The post-test probability is important for example in the case that the prevalence of a disease varies. For example: given a 90% sensitive test, the chances to find a diseased individual when screening 100 patients will depending on the prevalence (the prior or pre-test probability) of the disease in the particular population under study. When we apply the test to a population where our disease is present in 50% of the population, we will likely find 45 positive

100 Spiegelhalter DJ, Myles JP, Jones DR ,Abrams KR, Methods in health service research: An introduction to bayesian methods in health technology assessment BMJ. 1999; 319: 508-512.

test results. But if the frequency of this disease is 10%, applying the test to the same number of patients will give 9 positive results.

Probability revision is the process of converting the pre-test probability to the post-test probability taking the test result (the evidence) into account [101].

Post-test probabilities can be expressed in terms of the Bayes' formula:

(Equation 14) $$P(D+ \mid X) = \frac{P(D+) \times P(X \mid D+)}{P(D+) \times P(X \mid D+) + P(D-) \times P(X \mid D-)}$$

where *D*+ means presence of the disease and *D*- means absence of the disease and *X* means the finding after performing the test.

When we have a dichotomous test, the probability of a positive test result (*T*+) can be expressed as:

(Equation 15) $$P(D+ \mid T+) = \frac{P(D+) \times P(T+ \mid D+)}{P(D+) \times P(T+ \mid D+) + P(D-) \times P(T+ \mid D-)} =$$

$$= \frac{P(D+) \times Sensitivity}{P(D+) \times Sensitivity + P(D-) \times Specificity} \ ,$$

which is the Positive predictive value of the test.

And the probability of a negative test (*T*-) result can be expressed as:

(Equation 16) $$P(D+ \mid T-) = \frac{P(D+) \times P(T- \mid D+)}{P(D+) \times P(T+ \mid D+) + P(D-) \times P(T- \mid D-)} =$$

$$= \frac{P(D+) \times Specificity}{P(D+) \times Specificity + P(D-) \times Sensitivity} \ ,$$

which in fact is the Negative predictive value of the test.

As it has been stated before, when several tests have to be applied sequentially, we can use the posterior probabilities of the first test as the

101 Hunink MGM, Glasziou PP,Siegel J, Weeks J, Pliskin J, Elstein A, Weinstein M.Decision making in Health and Medicine, First Ed. 2001. Cambridge University Press, Cambridge, United Kingdom.

priors of our second test. In our case, if we would like to test whether MRS adds information to the MRI diagnosis, we would need the previous probability given by a diagnosis performed with MRI. ARTICLE 3 gives SE, SP, PPV and NPV that are directly usable in such studies.

8. CONCLUSIONS

1. The validated-DB complies with ethics regulations and is representative of the population studied. Its accessibility constitutes a European resource for neuroradiologists willing to use information provided by MRS to help in the non-invasive diagnosis of brain tumours and is currently being used in other European research projects, such as eTumour.
2. Short TE ^{1}H MRS (TE 30ms in this study) produces a slightly more accurate diagnostic outcome in general, whereas long TE (TE 136ms) is preferable when meningioma is suspected. From the clinical point of view, when only one spectroscopic sequence can be acquired, it would be preferable to use short TE except when a the presence of a meningioma is suspected. However, acquiring spectra at two different TE would be advisable whenever possible.
3. Neuroradiological classifications of human brain tumours with conventional MRI are highly specific and have variable SE. In some types, radiologists' phrasing pursues maximal SE and SP at the cost of not specifying the cellular origin of the tumour, such as in glial tumours. Studies aimed at proving the added value of MR-based techniques, should pursue to increase SE when specifying cell origin and grade of malignancy while retaining a high SP, especially for tumour types that are difficult to diagnose. The ground values for these

studies are provided by the post-test probabilities provided in the study presented in this thesis.

Annex 1. Fitting parameters used in Article 2

SHORT ECHO SPECTRA
Starting values

	frequency(ppm)	linewidth(Hz)
Naa;	2.02;	3.0;
Glx1;	2.11;	4.0;
Glx2;	2.2;	4.0;
Glx3;	2.29;	4.0;
Glx4;	2.36;	4.0;
Glx5;	2.43;	4.0;
Glx-NAA;	2.61;	6.0;
Cr;	3.03;	3.0;
Cho;	3.2;	3.0;
mI-Gly;	3.55;	3.0;
mI2;	3.64;	4.0;
Glx-Ala;	3.77;	4.0;
Glu;	3.83;	4.0;
Cr2;	3.91;	4.0;
Lip09;	0.9;	8.0;
Lip13;	1.25;	8.0;
Ala1;	1.4;	3.0;
Ala2;	1.52;	3.0;
Lac1;	1.3;	3.0;
Lac2;	1.38;	3.0;
sci;	3.33;	3.0;

Prior knowledge

Naa; amplitude -estimated; relative phase -fixed 0.0; linewidth -soft constraints ±0.1*WATlw;
Glx1; amplitude -estimated; relative phase -fixed 0.0; linewidth -fixed ratio Glx2*1.0;
Glx2; amplitude -estimated; relative phase -fixed 0.0; linewidth -soft constraints ±2*WATlw;
Glx3; amplitude -estimated; relative phase -fixed 0.0; linewidth -fixed ratio Glx2*1.0;
Glx4; amplitude -estimated; relative phase -fixed 0.0; linewidth -fixed ratio Glx2*1.0;
Glx5; amplitude -estimated; relative phase -fixed 0.0; linewidth -fixed ratio Glx2*1.0;
Glx-NAA; amplitude -estimated; relative phase -fixed 0.0; linewidth -soft constraints ±3.0*WATlw;
Cr; amplitude -estimated; relative phase -fixed 0.0; linewidth -fixed ratio Naa*1.0;
Cho; amplitude -estimated; relative phase -fixed 0.0; linewidth -fixed ratio Naa*1.0;
mI-Gly; amplitude -estimated; relative phase -fixed 0.0; linewidth -fixed ratio Naa*1.0;
mI2; amplitude -estimated; relative phase -fixed 0.0; linewidth -fixed ratio Glx-Ala*1.0;
Glx-Ala; amplitude -estimated; relative phase -fixed 0.0; linewidth -soft constraints ±2.0*WATlw;
Glu; amplitude -estimated; relative phase -fixed 0.0; linewidth -fixed ratio Glx-Ala*1.0;
Cr2; amplitude -estimated; relative phase -fixed 0.0; linewidth -fixed ratio Glx-Ala*1.0;
Lip09; amplitude -estimated; relative phase -fixed 0.0; linewidth -fixed shift Lip13+0.0
Lip13; amplitude -estimated; relative phase -fixed 0.0; linewidth -soft constraints ±3.0*WATlw;
Ala1; amplitude -estimated; relative phase -fixed 0.0; linewidth -fixed shift Naa+0.0;
Ala2; amplitude -fixed shift Ala1+0.0; relative phase -fixed 0.0; linewidth -fixed shift Naa+0.0;
Lac1; amplitude -estimated; relative phase -fixed 0.0; linewidth -fixed shift Naa+0.0;
Lac2; amplitude -fixed shift Lac1+0.0; relative phase -fixed 0.0; linewidth -fixed shift Naa+0.0;
sci; amplitude -estimated; relative phase -fixed 0.0; linewidth -fixed shift Glx-Ala+0.0;

Where WATlw is the value of the water linewidth obtained fitting the unsupressed water file with the HSVD algorithm.

Naa;	frequency -soft constraints 1.99-2.04;	shape -fixed Lorentzian;
Glx1;	frequency -soft constraints 2.1-2.14;	shape -fixed Lorentzian;
Glx2;	frequency -soft constraints 2.14-2.24;	shape -fixed Lorentzian;
Glx3;	frequency -soft constraints 2.24-2.34;	shape -fixed Lorentzian;
Glx4;	frequency -soft constraints 2.29-2.39;	shape -fixed Lorentzian;
Glx5;	frequency -soft constraints 2.34-2.44;	shape -fixed Lorentzian;
Glx-NAA;	frequency -soft constraints 2.54-2.69;	shape -fixed Lorentzian;
Cr;	frequency -soft constraints 2.98-3.08;	shape -fixed Lorentzian;
Cho;	frequency -soft constraints 3.17-3.27;	shape -fixed Lorentzian;
mI-Gly;	frequency -soft constraints 3.49-3.59;	shape -fixed Lorentzian;
mI2;	frequency -soft constraints 3.59-3.69;	shape -fixed Lorentzian;
Glx-Ala;	frequency -soft constraints 3.69-3.79;	shape -fixed Lorentzian;
Glu;	frequency -soft constraints 3.79-3.89;	shape -fixed Lorentzian;
Cr2;	frequency -soft constraints 3.84-3.94;	shape -fixed Lorentzian;
Lip09;	frequency -soft constraints 0.75-0.95;	shape -fixed Lorentzian;

```
Lip13;          frequency -soft constraints 1.15-1.35;      shape -fixed Lorentzian;
Ala1;           frequency -soft constraints 1.35-1.5;       shape -fixed Lorentzian;
Ala2;           frequency -soft constraints Ala1+7.0;       shape -fixed Lorentzian;
Lac1;           frequency -soft constraints 1.25-1.35;      shape -fixed Lorentzian;
Lac2;           frequency -soft constraints Lac1+7.0;       shape -fixed Lorentzian;
sci;            frequency -soft constraints 3.3-3.4;        shape -fixed Lorentzian;
```

Overall Phase

```
Zero order phase (deg): Fixed- Fixed value 0.0
Begin time (ms): Fixed- Fixed value 0.0
Weighting: On
Begin interval: 1, End: 20
Truncated points: 0
Points in Amares: 512
```

LONG ECHO SPECTRA
Starting values

	frequency(ppm)	linewidth(Hz)
Naa;	2.02;	3.0;
Glx1;	2.09;	4.0;
Glx2;	2.3;	4.0;
Glx3;	2.36;	4.0;
Glx4;	2.43;	4.0;
Glx-NAA;	2.61;	6.0;
Cr;	3.03;	3.0;
Cho;	3.2;	3.0;
mI-Gly;	3.55;	3.0;
Glx-Ala;	3.78;	4.0;
Lip09;	0.9;	8.0;
Lip13;	1.25;	8.0;
Ala1;	1.4;	3.0;
Ala2;	1.52;	3.0;
Lac1;	1.3;	3.0;
Lac2;	1.38;	3.0;
3.4;	3.42;	3.1;

Prior knowledge

```
Naa; amplitude -estimated; relative phase- fixed 0.0; linewidth- fixed ratio Cho*1.0;
Glx1; amplitude -estimated; relative phase- fixed 0.0; linewidth- fixed ratio Glx3*1.0;
Glx2; amplitude -estimated; relative phase- fixed 0.0; linewidth- fixed ratio Glx3*1.0;
Glx3; amplitude -estimated; relative phase- fixed 0.0; linewidth- estimated;
Glx4; amplitude -estimated; relative phase- fixed 0.0; linewidth- fixed ratio Glx3*1.0;
Glx-NAA; amplitude -estimated; relative phase- fixed 0.0; linewidth- estimated;
Cr; amplitude -estimated; relative phase- fixed 0.0; linewidth- fixed ratio Cho*1.0;
Cho; amplitude -estimated; relative phase- fixed 0.0; linewidth- estimated;
mI-Gly; amplitude -estimated; relative phase- fixed 0.0; linewidth- fixed ratio Cho*1.0;
Glx-Ala; amplitude -estimated; relative phase- fixed 0.0; linewidth- fixed ratio Cho*1.0;
Lip09; amplitude -estimated; relative phase- fixed 0.0; linewidth- fixed shift Lip13+0.0;
Lip13; amplitude -estimated; relative phase- fixed 0.0; linewidth- estimated;
Ala1; amplitude -estimated; relative phase- fixed 180.0; linewidth- fixed shift Cho+0.0;
Ala2; amplitude -fixed shiftAla1+0.0; relative phase- fixed 180.0;linewidth- fixed shift Cho+0.0;
Lac1; amplitude -estimated; relative phase- fixed 180.0; linewidth- fixed shift Cho+0.0;
Lac2; amplitude -fixed shiftLac1+0.0; relative phase- fixed 180.0;linewidth- fixed shift Cho+0.0;
3.4; amplitude -estimated; relative phase- fixed 0.0; linewidth- fixed ratio Cho*1.0;
```

```
Naa;            frequency- soft constraints 1.99-2.04;      shape- fixed Lorentzian;
Glx1;           frequency- soft constraints 2.05-2.14;      shape- fixed Lorentzian;
Glx2;           frequency- soft constraints 2.24-2.34;      shape- fixed Lorentzian;
Glx3;           frequency- soft constraints 2.29-2.39;      shape- fixed Lorentzian;
Glx4;           frequency- soft constraints 2.34-2.44;      shape- fixed Lorentzian;
Glx-NAA;        frequency- soft constraints 2.54-2.69;      shape- fixed Lorentzian;
Cr;             frequency- soft constraints 2.98-3.08;      shape- fixed Lorentzian;
Cho;            frequency- soft constraints 3.17-3.27;      shape- fixed Lorentzian;
mI-Gly;         frequency- soft constraints 3.5-3.6;        shape- fixed Lorentzian;
Glx-Ala;        frequency- soft constraints 3.73-3.83;      shape- fixed Lorentzian;
Lip09;          frequency- soft constraints 0.7-1.0;        shape- fixed Lorentzian;
Lip13;          frequency- soft constraints 1.2-1.4;        shape- fixed Lorentzian;
Ala1;           frequency- soft constraints 1.35-1.5;       shape- fixed Lorentzian;
Ala2;           frequency- fixed shift Ala1+7.0;            shape- fixed Lorentzian;
Lac1;           frequency- soft constraints 1.25-1.35;      shape- fixed Lorentzian;
Lac2;           frequency- fixed shift Lac1+7.0;            shape- fixed Lorentzian;
3.4;            frequency- soft constraints 3.35-3.45;      shape- fixed Lorentzian;
```

Overall Phase

Zero order phase (deg): Fixed - Fixed value 0.0;
Begin time (ms): Fixed- Fixed value 0.0;
Weighting: On
Begin interval: 1, End: 20;
Truncated points: 0
Points in Amares: 512

Note

If estimated linewidth of:

Glx2 is > 2.0*Cho linewidth value,
Lip09 is > 3.0*Cho linewidth value,
Lip13 is > 3.0*Cho linewidth value,
Glx-Naa > 3.0*Cho linewidth value,

Then: run AMARES again using the following soft constraints:

Glx2 linewidth- 2.0*Cho linewidth value,
Lip09 linewidth- 3.0*Cho linewidth value,
Lip13 linewidth- 3.0*Cho linewidth value,
Glx-Naa linewidth- 3.0*Cho linewidth value.